Relaxation Dynamics in Mixtures of Long and Short Chains: Tube Dilation and Impeded Curvilinear Diffusion

Shanfeng Wang, Shi-Qing Wang,* A. Halasa, and W.-L. Hsu†

Maurice Morton Institute of Polymer Science and Department of Polymer Science, University of Akron, Akron, Ohio 44325

Received July 2, 2002; Revised Manuscript Received April 21, 2003

ABSTRACT: A theoretical and experimental investigation of relaxation dynamics is carried out for binary mixtures of entangled short and long chains of the same species. In disagreement with the previous theories of Doi et al. [*Macromolecules* **1987**, *20*, 1900] and Viovy et al. [*Macromolecules* **1992**, *24*, 3587], the new experimental data indicate that the terminal relaxation time associated with the long chains decreases systematically with the short chain length and with the weight fraction ϕ of the long chains for all the mixtures. These experimental observations have inspired the proposal of a new reptation theory to account for (1) the tube dilation (TD) due to the constraint release by short chains, (2) impedance of the long chain's curvilinear diffusion, and (3) enhanced contour length fluctuation, all resulting from the incorporation of the short chains of length N_S. The various increases of the long chain's relaxation rate with lowering ϕ for its mixtures with different short chain lengths are possible only if the long chain reptates in a dilated tube of a shorter contour length with a curvilinear diffusivity that depends nontrivially on ϕ and N_S. The short chain's influence on the long chain's curvilinear diffusion, characterized by an impedance function λ that explicitly depends on N_S and ϕ, is demonstrated by comparison between the theory and experiment. Finally, the contour length fluctuation (CLF) is found to be enhanced in the binary mixtures and to produce additional concentration dependence for the terminal relaxation time; i.e., the CLF correction is larger at lower concentrations and for lower molecular weights of the long chains.

I. Introduction

Dynamics of entangled polymer solutions, melts, and blends are a subject of lasting importance because of their relevance to many physical phenomena and properties including polymer diffusion, phase separation, viscoelasticity, and processing. The task of determining the chain disentanglement times is an intrinsically many-body problem that is so far intractable. A key simplification was introduced in the early days of the theoretical development by formulating a mean-field description of such a complex system.[1,2] Within this popular model of tube-confined reptation, the dynamic motion of a probe chain (also known as the primitive chain) is depicted to take place in a tube that represents the mean-field average effect of all other chains on the diffusive movement of the primitive chain. A simple scaling law arises straightforwardly in this theory of de Gennes, Doi, and Ewards for the terminal relaxation time τ_{d0} and (zero-shear) melt viscosity η_0 as a function of molecular weight for a melt of uniform chain length: $\tau_{d0} \propto \eta_0 \propto M_w^3$, where the subscript "d0" denotes disentanlgement in monodisperse melts. Although experimental data display a slightly larger exponent around 3.4, this initial result has been regarded as a great theoretical triumph.

As detailed in the next section, many modifications have been introduced to bring the original theory into better accord with experiment. For monodisperse melts, it has been established[2] that the reptation model offers a satisfactory account of the experimental observations upon incorporation of the contour length fluctuation effect.[3] Going beyond the simplest case of monodisperse melts, many workers[4−10] explored the relaxation dynamics of mixtures of long and short chains, i.e., melts with a bimodal molecular weight distribution, as the first step toward a full understanding of rheology of polydisperse samples. The last major theoretical attempt to formulate a rigorous reptation theory for such mixtures was carried out over a decade ago.[11] Despite the efforts that have lasted nearly two decades, there are insufficient experimental studies to systematically examine the influence of short chains on the disentanglement dynamics of the long chains for different short chain lengths at all compositions. Consequently, an explicit comparison between theory and experiment has been largely unavailable.[12,13]

In the past decade or so, there has been a lot of interest in arriving at various theoretical descriptions of polymer rheology for entangled polydisperse melts. Many of these studies[14−18] are motivated by the idea of double reptation.[19−21] Unlike the theory of Viovy et al.[11] that focused on concepts and mechanisms, these papers have placed on an emphasis on numerical prediction of the master curves for G' and G''.

Recently, the chain dynamics in heterogeneous mixtures of long and short chains have been experimentally studied where the long and short chains are of different species and the long chains dominate the terminal relaxation.[22] The objective was to probe the friction dynamics of component A in the presence of component B and vice versa as a function of temperature and composition. In our previous work,[22] the short chain was marginally entangled to avoid the complication associated with the coupling of dynamics between long and short chains. Since short chains of length N_S typically have a lower glass transition temperature than that of the long chains until $N_S > N_e$ (entanglement chain length), for this solution rheology approach to be reliable quantitatively it is desirable to first work out the influence of short chains on the relaxation dynamics of

† Chemical Division Research and Development, Goodyear Tire and Rubber Company, Akron, OH 44305.

* Corresponding author: e-mail swang@uakron.edu.

10.1021/ma0210426 CCC: $25.00
Published on Web 06/10/2003

long chains in a homo-mixture of long and short chains where N_S is appreciably larger than N_e.

The objective of this work is to study the terminal relaxation dynamics of a binary mixture of the same species as a function of composition for different long and short chain lengths. In particular, we have carried out systematic oscillatory shear measurements of the disentanglement times of the long chains as a function of the short chain length at different compositions based on monodisperse 1,4-polybutadiene melts. After reviewing the key theoretical ideas of the standard reptation theory that have been put forward over the past 20 years and examining the previous theories[11,23] that represent the status of the current theoretical understanding, we present our new theoretical model for binary mixtures in section II, which is inspired by our own experimental data that follows in section IV. The comparison between our theory and experiment reveals that entangled short chains affect the long chain's overall relaxation in three ways: (a) dilating the tube that confines the probe long chain, (b) impeding the curvilinear diffusion of the long chain in the dilated tube, and (c) enhancing the effect of contour length fluctuation. This new reptation theory rectifies the previous analytical descriptions and should stimulate new experiments, computer simulations, and further theoretical development. As discussed below, this model is applicable on the basis of the notion of tube dilation, which is a useful idea when there is a wide separation in respective time scales associated with long and short chains.

II. Reptation Theory

In this theoretical section, we briefly review and comment on the concepts of *contour length fluctuation*, *constraint release*, and *tube dilation* in section II.A before examining the previous theories[11,23] on terminal dynamics of binary entangled mixtures in section II.B. A more detailed description of the standard tube model can be found in refs 12 and 13. After pointing out the discrepancies between the previous theories and our experimental data, we present a new theoretical formulation in section II.C. The detailed comparison between experiment and theory in section V will underscore the objective of the present study. To maintain clarity, we will omit numerical prefactors throughout the presentation and discussion of the theoretical results in this paper. Those familiar with the previous reptation theories can directly skip to section II.C.

A. Various Factors beyond Original Tube Model.

1. Contour Length Fluctuation. The mean-field reptation theory, developed by de Gennes,[1] Doi, and Edwards,[2] has proved to be an insightful and successful description of entanglement dynamics of linear polymer chains. In a fixed tube of diameter a and length L formed by other chains, the longest chain relaxation time (i.e., disentanglement time) $\tau_{d0} \simeq L^2/D_c$ is argued to scale with the chain length N as $\tau_{d0} \propto N^3$, in approximate agreement with the experimental results[24] $\tau_0 \propto N^{3.4}$, where the Rouse diffusion coefficient is related to the segmental friction constant ζ as[24]

$$D_c(N) = k_B T/\zeta N \equiv b^2/\tau N \tag{1}$$

with b being the Kuhn segmental length, and the contour length L proportional to N, where the second equality defines the elemental time τ. The most important correction to the original theory is the incorporation of the contour length fluctuation effect (CLF),[3] now well accepted as the key ingredient that revises the exponent from 3 to 3.4 for the molecular weight scaling of the disentanglement relaxation time. The CLF effect leads to an effective contour length

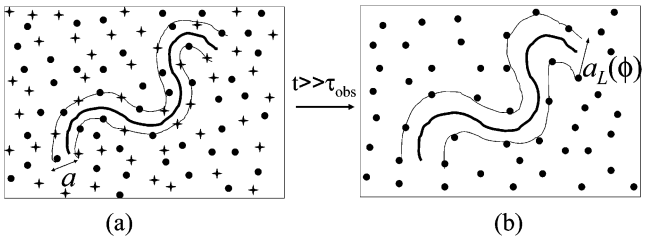

Figure 1. (a) Schematic of a probe long chain confined in the bare tube of diameter a when $t \leq \tau_{obs}$, where other long and short chains are symbolized by circles and crosses, respectively. In the single chain limit (i.e., few long chains in a matrix of short chains), all symbols would be taken as representing the short chains. (b) When $\tau_d > t \gg \tau_{obs}$, the short chains release their constraint to allow the probe chain to reptate in a dilated tube of diameter $a_L(\phi)$.

$$L_{CLF} = L[1 - X(a/R)] \tag{2a}$$

modifying the disentanglement time to[2]

$$\tau_{d0}^{CLF}(N) \simeq {L_{CLF}}^2/D_c \simeq \tau_{d0}(N)[1 - X(N_e/N)^{1/2}]^2 \tag{2b}$$

where the numerical factor X is taken as 1.45 in this paper, N_e denotes the entanglement chain length, related to the tube diameter as $a = \sqrt{N_e}b$, R is the average chain size equal to $\sqrt{N_e}b$, and the original disentanglement time $\tau_{d0}(N)$ is

$$\tau_{d0}(N) \simeq L^2/D_c = \tau_e(N/N_e)^3 \simeq \tau_R(N/N_e) \tag{2c}$$

where the elementary time $\tau_e = \tau N_e^2$ corresponds to the length scale of the tube diameter a, with τ related to the Rouse diffusion constant D_c according to eq 1, and

$$\tau_R(N) \simeq R^2/D_c = \tau_e(N/N_e)^2 = \tau N^2 \tag{2d}$$

is the Rouse relaxation time.[2]

2. Constraint Release. Constraint release (CR), also known as tube reorganization, was the first idea introduced[25−27] after the initial reptation model to recognize the fact that all of the other chains forming the tube for the probe chain are also mobile even for a monodisperse sample. The CR effect is found to yield an insignificant correction to the pure reptation when N/N_e is much larger than one. The concept of CR becomes very useful and important to incorporate for polydisperse samples. The situation is most straightforward in the single chain limit, whereas the next simplest case of binary mixtures with a comparable amount of long and short chains is still poorly understood and is the subject of this work. We start with a discussion of the dilute limit and defer the more complicated problem of binary mixtures to the last subsection. Let us picture a long probe chain immersed in a matrix of short chains as depicted in Figure 1a, where the two symbols are for the time being both taken to be identical in terms of confining the probe chain with the same lifetime τ_{obs} to the bare tube as indicated by the thin lines. For these short chains, the CR correction to the original eq 2c for the disentanglement time may

be significant and therefore needs to be incorporated according to Klein[25] as

$$\tau_{obs}(N_S) \simeq \tau_{d0}^{CLF}(N_S)/[1 + A(N_e/N_S)^2] \qquad (3a)$$

where A is a constant around 10 and the CLF effect is incorporated. The embedded long chain would diffuse about in a Rouse-like fashion with a coarse-grained elementary step length equal to $a = \sqrt{N_e}b$ and elementary time scale equal to τ_{obs} given by eq 3a, with a relaxation time τ_R^{CR} resembling eq 2d

$$\tau_R^{CR}(N_L,N_S) \simeq \tau_{obs}(N_S)(N_L/N_e)^2 \simeq \gamma(N_S)\,\tau_R(N_L) \qquad (3b)$$

where the subscript "R" in τ_R^{CR} is to remind us of the Rouse-like dynamics executed by the long chain and τ_R is the Rouse relaxation time in eq 2d for the long chain. Here a new parameter γ naturally arises, given by

$$\gamma(N_S) \equiv \tau_{obs}(N_S)/\tau_e \simeq (N_S/N_e)^3[1 - X(N_e/N_S)^{1/2}]^2/[1 + A(N_e/N_S)^2] \qquad (3c)$$

which can be rather large when N_S/N_e is greater than unity.

The center-of-mass diffusion of a long chain in a matrix of short chain can be quantified by a self-diffusion constant D^{CR} that is related to the relaxation time of eq 3b as

$$D^{CR}(N_L,N_S) \simeq R^2/\tau_R^{CR} \simeq D_c/\gamma = (3/\alpha)D_G \qquad (4a)$$

where the second equality follows from $D_c \simeq R^2/\tau_R$ and the third equality, following from use of the expression for the center-of-mass diffusion coefficient in the pure melt (using eq 6.40 of ref 2), $D_G = (D_c/3)(N_e/N_L)$, defines the new parameter α as

$$\alpha(N_L,N_S) \equiv (N_e/N_L)\gamma(N_S) \simeq \tau_R^{CR}(N_L,N_S)/\tau_{d0}(N_L) \qquad (4b)$$

which is the same as introduced by Viovy et al.[11] as the ratio of the two relaxation times given by eqs 3b and 2c, respectively, and is identical to the reciprocal of the Struglinski−Graessley parameter,[28] aside from the additional CLF and CR correction factors. Equation 4a indicates that the diffusive movement of the long chain in a matrix of entangled short chains is impeded by a factor of γ relative to that of the free Rouse diffusion characterized by D_c. The same scaling relation as eq 4a has been available since 1979.[1] We can also simply derive eq 4a for D^{CR} by analogy to eq 1: $D^{CR} \simeq a^2/\tau_{obs}(N_L/N_e)$. Finally, when $\alpha \gg 1$ such a long chain is expected to execute the Rouse-like diffusive motion with a diffusion coefficient D^{CR} that is smaller than D_G governing the self-diffusion of the long chain in its pure melt, implying the long chain would diffuse in a matrix of short chain length N_S with a rate identical to that found for the monodisperse melt of long chains. It is necessary to note that the results presented in this subsection II.A.2 are only valid in the single long chain limit and need modification when used to formulate the theory for binary mixtures. Specifically, at finite weight fractions of the long chains, there is little CR effect thanks to the long chains, i.e., the CR factor, $[1 + A(N_e/N_S)^2]^{-1}$, can be dropped from eq 3c.

3. Tube Dilation and Terminal Plateau Modulus. Although the original notion of *tube dilation* (TD) was first introduced by Marrucci[29] to acknowledge the mobile nature of the tube that confines the entangled chains in polymer melts, its literal meaning is most unambiguously clear and useful to depict the chain dynamics of entangled polymer *solutions*. In comparison with the undiluted counterpart, a chain in an entangled solution reptates in a dilated tube whose diameter a_L is related to the terminal plateau modulus $G_{pl}(\phi)$ according to[22,30]

$$G_{pl}(\phi) = G_N^0\phi[a/a_L(\phi)]^2 \qquad (5a)$$

where G_N^0 is the plateau modulus of the monodisperse polymer melt. There have been theoretical speculations[31] based on scaling analyses of how the enlarged diameter $a_L(\phi)$ changes with ϕ in this case of *ideal* tube dilation in polymer solutions. At high concentrations where the long chains assume Gaussian statistics, we may expect the scaling of $a_L(\phi)$ with ϕ to be nearly universal independent of the solvent quality. Experimentally, it has been found previously for solutions where the "solvent" is an oligomeric melt,[22] for binary mixtures,[28] and again in the present work that

$$G_{pl}(\phi)/G_N^0 = \phi^{2.2} \qquad (5b)$$

implying that $a/a_L(\phi) \propto \phi^{0.6}$.

For *monodisperse* entangled linear melts, the original concept of dynamic tube dilation has not found much usefulness although it has been successfully applied to describe the dynamics of branched polymer melts.[32]

For entangled binary mixtures where the long chains relax much more slowly than the short chains, the *same* suppressed terminal plateau modulus as described by eqs 5a and 5b for solutions has been found both previously[28] and in the present work. It is in this sense that tube dilation (TD) is ubiquitous for polydisperse melts and particularly easy to identify for the simplest case of binary mixtures.

Although previous theories[11,23] all anticipated the suppression of the terminal plateau as depicted by eqs 5a and 5b and the corresponding tube dilation, they do not agree on whether and under what conditions such a constraint release by the short chains would result in speeding up the long chain's terminal relaxation relative to that in the pure long chain melt. Specifically, different arguments were made to address the question of *whether and how* the long chain would literally reptate in the dilated tube of diameter a_L, which is related to the terminal plateau modulus through eq 5a. Despite the constraint release by the short chains that leads to eq 5a and the visualization of the corresponding tube dilation, both theories of Doi et al.[23] and Viovy et al.[11] asserted that the long chains would still reptate in the skinny bare tube of diameter a whenever α of eq 4b is greater than unity. These various points of view will be assessed in detail in section II.B.

In this paper, we visualize a mixture of long and short chains represented by circles and crosses respectively as shown in Figure 1a where the crosses are *much more mobile* than the circles. Suppose the short and long chains' disentanglement times are $\tau_{obs}(N_S)$ and τ_d, respectively. For $\tau_d > t \gg \tau_{obs}$, the short chains move away to release their constraint on the probe long chain, and only long chains still confine the probe chain. Pictorially speaking, we can visualize the short chains' CR at these long times by removing the crosses from

Figure 1a as shown in Figure 1b. In other words, well beyond τ_{obs} the tube dilation (TD) would take place as depicted in Figure 1b. Suppose the weight fraction of the long chains is ϕ; the consequence of TD from the bare tube diameter a to $a_L(\phi)$ is that the tube or contour length shrinks from L to $L(\phi)$ according to

$$L(\phi)\, a_L(\phi) = R^2 = La \tag{6}$$

The long chain is now envisioned to reptate in this shorter swollen tube of length $L(\phi) < L$ with a curvilinear diffusivity that is yet to be specified. This notion of tube dilation will be developed in detail in section II.C and in section IV, where we will elucidate that this tube dilation is an important and useful concept in the theoretical description of binary mixtures of linear chains and takes place more frequently than previously expected.

B. Previous Theories for Chain Dynamics of Binary Mixtures. *1. Tube Dilation Model of Doi−Graessley−Helfand−Pearson.* The first serious theoretical attempt to describe the polymer dynamics in polydisperse melts was made by Doi et al.[23] Following the initial idea of Marrucci,[29] these workers derived the condition under which the long chains in a binary mixture would *reptate* in a dilated tube. Picturing a long chain of length N_L in a matrix of short chains of length N_S, it was proposed that the times scales to compare with are the lifetime of the obstacle, $\tau_{obs}(N_S)$ of eq 3a, and the time required for the long chain to diffuse a distance equal to the bare tube diameter a, i.e., a^2/D_c. The ratio of these two times is precisely the parameter $\alpha(N_L,N_S)$ of eq 4b. It was asserted that when $\alpha > 1$ the short chains would effectively confine the long chain to the extent that the long would only reptate in the bare tube of diameter a and would disentangle only at $\tau_{d0}^{CLF}(N_L)$ of eq 2b. In other words, the relaxation of a long chain would not be accelerated, relative to its relaxation in the pure long chain melt, by the short chains when $\alpha(N_L,N_S) > 1$.

This same argument has since been echoed by several authors.[12,13,15] On the basis of their experimental data on binary mixtures, Struglinski and Graessley[28] concluded that the terminal relaxation time of the long chains in the mixtures with $\alpha > 1$ at different compositions was indistinguishable from that found in the pure long chain melt. This result has been reviewed as the supporting evidence that the long chains do not reptate in the dilated tube but in the bare tube instead. In the present paper, we have examined mixtures comparable to those studied by Struglinski and Graessley and found a discernible shift of the terminal relaxation time with the composition.

There are several limitations in the theoretical treatment of Doi et al.,[23] the least of which is that it neglects to consider whether the short chains would provide an effective tube confinement at times much longer than $\tau_{obs}(N_S)$ during the long chain's journey to disentangle at $\tau_{d0}^{CLF}(N_L) \gg \tau_{obs}(N_S)$. We will examine in section IV using our experimental data whether the long chains would indeed relax as slowly in a binary mixture with $\alpha > 1$ as in the pure long chain melt. When $\alpha < 1$, Doi et al.[23] suggested that the long chain would reptate in the dilated tube whose diameter would be a_L revealed in eq 5a, with a curvilinear diffusivity equal to the Rouse diffusivity D_c of eq 1. This led to the prediction that the long chain's relaxation time, although dependent on the composition ϕ due to the shrunk tube length according to eqs 6 and 5b, would *not* depend on the short chain length N_S. Again the experimental data to be presented in section IV are in disagreement with this prediction.

2. Supertube Model of Viovy−Rubinstein−Colby (VRC). The Viovy−Rubinstein−Colby theory[11] compared the time $\tau_R^{CR}(N_L,N_S)$ of eq 3b associated with the tube reorganization allowed by the constraint release of the short chains with the long chain's disentanglement time $\tau_{d0}(N_L)$ of eq 2c to arrive at the α parameter given in eq 4b. It reached the same conclusion as that of the Doi et al.'s theory[23] that the long chain's terminal relaxation time would be not accelerated by the constraint release of the short chains for $\alpha > 1$.

By comparing the obstacle's lifetime $\tau_{obs}(N_S)$ and the time $\tau_e = \tau N_e^2$ beyond which the probe chain would feel the tube confinement, Viovy et al. concluded[11] that the long chain would reptate in the dilated tube with curvilinear diffusivity D_c of eq 1 only when $\gamma < 1$ or essentially when $N_S < N_e$, in contrast to the condition of $\alpha < 1$ advocated by Doi et al.[23] It was asserted that when $\gamma > 1$ and $\alpha < 1$, the long chain would always be confined to the bare tube of diameter a, and this *tube* would reptate in the *supertube* of the dilated diameter a_L, with the elemental length and time scales being a and τ_{obs}, respectively. This amounts to the long chain reptating in the dilated tube with a curvilinear diffusivity equal to $D^{CR}(N_L,N_S) = a^2/\tau_{obs}(N_S)(N_L/N_e)$ of eq 4a. On the basis of these arguments, the time for "tube disentanglement" from the supertube can be readily derived in one step as

$$T_{rep}^{tube}(N_L,N_S,\phi) \simeq L^2(\phi)/D^{CR}(N_L,N_S) \simeq \tau_{d0}(N_L)(a/a_L)^2\gamma(N_S) \tag{7}$$

where the second equality follows from use of eqs 2c, 4a, and 6, and γ is given by eq 3c. Equation 7 is the result given in eqs 20 and 22 in ref 11, aside from the CLF and CR factors in eq 3c. One important assumption of the theory was that the overall chain relaxation occurs, at finite concentrations of the long chains, via *two independent* processes: (a) the bare tube reptation in the dilated tube (i.e., the supertube) and (b) the "ordinary chain reptation in the bare tube of diameter a".[11]

There are several key results in this VRC theory to be summarized here. (I) Like the theory of Doi et al.,[23] when $\alpha > 1$ in eq 4b, the pure chain reptation is expected to dominate. (II) When $\alpha < 1$ in eq 4b but $(a/a_L)^2\gamma(N_S) > 1$, the tube reptation in the supertube is too slow and the long chains would relax by the pure chain reptation. (III) Under other circumstances, eq 7 depicts the long chain's relaxation dynamics, and the ϕ dependence of the terminal relaxation time is the same as given by the ideal tube dilation, i.e., by $(a/a_L)^2$, independent of N_S. Moreover, the VRC theory dictates that the terminal plateau width is independent of N_S and is identical to that of an entangled solution where ideal tube dilation is present. Although some experimental observations exist in the literature,[4−10] there have been no systematic data to contest these previous theories. One purpose of this work is to provide a comprehensive set of experimental data to scrutinize the existing theoretical descriptions and to inspire new theoretical development.

C. New Model. The data to be presented in Figure 9b in section IV appear to contradict explicitly with the basic predictions of the previous theories: Even when

$\alpha \gg 1$ (e.g., for 410K/44K mixtures), the terminal relaxation time is still shorter than that of the pure melt of long chains even at finite concentrations. When $\alpha < 1$, the weight fraction dependence of terminal relaxation time τ_d associated with the long chains is not universal but rather dependent on the short chain length N_S in contrast to the prediction of Doi et al.,[23] indicated by the inclined line. Our data also seem to disagree with prediction II of Viovy et al.[11] depicted by the horizontal line since τ_d is found to be smaller than that of the pure long chain melt even under the condition of $(a/a_L)^2\gamma(N_S) \gg 1$, which holds for mixtures 410K/12K, 410K/8.9K, and 410K/5.8K for most values of ϕ.

The disagreement between the experiment and the previous theories begins at a conceptual level. One objective of this work is to build a new theoretical formulation *within* the framework of a tube model and to offer a successful phenomenological account of the experimental observations. It is important to point out at the onset that our theoretical description is applicable only when there is a wide separation of time scales associated with the long and short chains. Under this condition, entanglement spacing is enlarged at long times (i.e., in the terminal region) due to the constraint release by the short chains. This enables the convenient notion of tube dilation to be used in building a tube model for such binary mixtures. Within this model the long chain diffuses in an effective tube of dilated diameter a_L, which is related to the terminal plateau modulus as shown in eq 5a. We expect the model to gradually become inaccurate for mixtures where the disentanglement time of short chains is too close to that of the long chains. When the terminal plateau width shrinks to 2 decades, it is perhaps not even accurate to determine the terminal relaxation time from the oscillatory shear measurements.

1. Terminal Relaxation Time. In this work, we propose to formulate a new reptation theory that explicitly incorporates both TD and enhanced CLF effects and accounts for the CR process affecting the curvilinear diffusion in the dilated tube. Our model only addresses the situation where there is a clear separation of time scales (i.e., at least 3 decades) in binary mixtures associated with the long and short chains respectively, so that the tube dilation is a prevailing process; i.e., the long chains literally relax by reptation in a dilated tube. We first introduce an effective contour length of the primitive chain in the dilated tube of diameter a_L

$$L_{CLF}(\phi) = L(\phi)[1 - X(a_L/R)] \tag{8}$$

which is a simple extension of eq 2a, where $L(\phi)$ has been introduced in eq 6 in the previous subsection II.A.3 on tube dilation. Second, we envision the long chains to diffuse in an effective medium whose structure depends on the composition and short chain length N_S. In other words, the long chains are expected to reptate in a dilated tube of diameter a_L with a curvilinear diffusivity $D(N_L,N_S,\phi)$ that vary with N_S and ϕ due to the constraint release effect of the short chains apart from its linear dependence on N_L. In contrast to the VRC theory where two dynamic processes of pure chain reptation and tube reptation in the supertube are thought to occur independently, in our model the long probe chain reptating in an effective medium of the short-chain-dilated tube is the *only* process for relaxation. Provided that the long chains are still entangled with one another, we have a simple expression for the disentanglement time of the long chain in the presence of short chains

$$\tau_d(N_L,N_S,\phi) \simeq L_{CLF}^2(\phi)/D(N_L,N_S,\phi) \simeq \tau_d^{TD}(N_L,\phi)\,\lambda(N_S,\phi) \tag{9a}$$

where the relaxation time due only to the ideal tube dilation is given by

$$\tau_d^{TD}(N_L,\phi) \simeq \tau_{d0}(a/a_L)^2[1 - X(a_L/a)(N_e/N_L)^{1/2}]^2 \tag{9b}$$

and the impedance parameter λ accounts for the constraint release effect of the short chains on the curvilinear diffusivity and is defined as

$$\lambda(N_S,\phi) = D_c(N_L)/D(N_L,N_S,\phi) \tag{9c}$$

with D_c (given by eq 1) being the curvilinear diffusivity of the long chain in its bare tube in the pure long chain melt. By definition, λ is independent of the long chain length N_L and has to satisfy two limits. In the limit of $\phi = 1$, $\lambda = 1$. As ϕ decreases, D might approach something like D^{CR} of eq 4a, i.e., λ becoming strongly N_S dependent and eventually proportional to γ. Therefore, at a given ϕ, λ is expected to increase with N_S, and at a fixed N_S, λ is expected to increase with decreasing ϕ. At low enough ϕ where the long chains are no longer entangled with one another, the concept of λ being related to the curvilinear diffusivity would no longer be valid. Throughout this paper, we consider only highly entangled mixtures where the diluent is a melt of short chain of length N_S and the long chains are highly entangled with one another. When the diluent is a small molecule solvent, λ is expected to depend on the solvent viscosity η_s in some nontrivial way. We will return to eqs 9a−9c in section V.

It is important to note that the diffusion coefficient D in eqs 9a and 9c depicts the mobility of the primitive long chain in the *dilated tube* where the short chains participate in hindering the curvilinear diffusion of the long chain on the spatial scale defined by the diameter a_L of the dilated tube, which varies with the composition ϕ.

2. Intrachain Dynamics: Segmental Displacement. (i) Entangled Short Chain. The description for chain dynamics at short times is analogous to that given in ref 2 but fundamentally different from that of ref 11. We will provide a graphic representation in Figure 2, which is analogous to Figure 6.10 of ref 2. At very short times before the bare tube confinement is felt, the probe long chain is like a free Rouse chain inside a tube of diameter a. In terms of the mean-square displacement $\Phi(t)$ of a chain segment, we have

$$\Phi(t) \simeq b^2(t/\tau)^{1/2}, \quad \tau < t \le \tau_e \tag{10}$$

where the elemental times τ and τ_e have been defined in eqs 1 and 2d, respectively. For $t > \tau_e$, the long chain can only move along the primitive path within the bare tube (as shown in Figure 1a) defined by short and long chains until the short chains diffuse away at an obstacle time τ_{obs} given in eq 3a. Namely

$$\Phi(t) \simeq a^2(t/\tau_e)^{1/4}, \quad \tau_e < t \le \tau_{obs} \tag{11}$$

So far, the physics is the same as outlined in ref 2. Beyond τ_{obs} and at times that are multiples of τ_{obs}, the

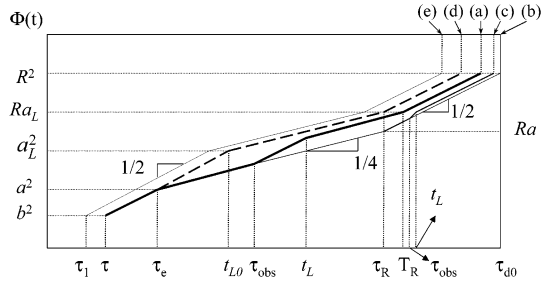

Figure 2. Mean-square displacement $\Phi(t)$ of the long chain segment as a function of time under five different conditions in a double-logarithmic plot. (a) The thick lines depict the full dynamics of a probe long chain in a binary mixture of long and short chains for $\tau_R > \tau_{obs}$ where the short chains dilate the bare tube of diameter a to a diameter of a_L. The disentanglement time τ_d is reached at $\Phi(\tau_d) = R^2$. (b) In contrast, the thin lines below the thick ones ending at τ_{d0} are for the case of a pure long chain melt as given in Figure 6.10 of ref 2. (c) For $\tau_{obs} > \tau_R$, the dynamics deviate from that of the pure reptation after τ_{obs} when the probe chain starts free Rouse movement, become confined by the dilated tube at t_L, and reach disentanglement at τ_d. (d) The dashed lines are $\Phi(t)$ for the case of ideal tube dilation where the marginally entangled short chains (i.e., $N_S = N_e$) only dilate the tube without impeding the curvilinear diffusion so that the disentanglement time is τ_d^{TD} given by eq 9b. (e) The thin lines above the dashed lines describe $\Phi(t)$ for a polymer "solution" where the diluent is either a melt of unentangled short chains or solvent of small molecules and the dynamics are accelerated on all time scales starting with the elemental time $\tau_1 < \tau$.

bare tube is no longer felt by the probe long chain due to the constraint release by the short chains. Below we consider a coarse-grained picture where the long chain would reptate in the dilated tube with a mobility that is dependent on the short chain's disentanglement time τ_{obs} and the tube diameter a_L, as depicted in Figure 1b. The impeded Rouse-like motion is described by the following expression

$$\Phi(t) \simeq \gamma^{1/4} a^2 (t/\tau_{obs})^{1/2}, \quad \tau_{obs} < t \le t_L \tag{12}$$

which comes to an end when the primitive long chain meets at t_L the confinement of other long chains at the "wall" of the dilated tube. In eq 12 γ is defined in eq 3c, and t_L is yet to be specified. Beyond t_L, the long probe chain is confined within the dilated tube that is "filled with" short chains impeding the long chain's mobility. The motion of the Rouse segment perpendicular to the primitive path of the dilated tube is now restricted; thus, $\Phi(t)$ scales as $t^{1/4}$ as

$$\Phi(t) \simeq \gamma^{1/4} a^2 (t_L/\tau_{obs})^{1/2} (t/t_L)^{1/4}, \quad t_L < t \le T_R \tag{13}$$

similar to the first line of eq 6.109 in ref 2. We assign the diffusion coefficient D introduced in eq 9a to depict the impeded Rouse motion of the long chain in the coarse-grained medium of the dilated tube such that the impeded Rouse time T_R in eq 13 is related to D as

$$T_R(N_L,N_S,\phi) \simeq R^2/D \simeq \lambda(N_S,\phi)\, \tau_R(N_L) \tag{14}$$

where λ and τ_R have been defined in eqs 9c and 2d, respectively. Finally, above T_R the long time behavior of the impeded Rouse dynamics dictates so that

$$\Phi(t) \simeq a_L (Dt)^{1/2}, \quad T_R \le t \le \tau_d \tag{15}$$

which is similar to the second line of eq 6.109 in ref 2. Φ reaches R^2 when the long chain disentangles at $\tau_d \simeq (R^2/a_L)^2/D$, which is the same as the result in eqs 9a−c apart from the CLF correction.

Since $\Phi(T_R) = Ra_L$ follows from inserting eq 14 into eq 15, we can equate it with the expression of eq 13 at T_R to identify the confinement time t_L to be

$$t_L = (\tau_{obs}/\lambda)(a_L/a)^4 = (\gamma/\lambda) t_{L0} \tag{16a}$$

where $t_{L0} = \tau_e (a_L/a)^4$ is the confinement time for the dilated tube when $N_S = N_e$. t_L is an important time scale and is when the long chain begins to experience the confinement of the dilated tube (i.e., the constraint exerted by the other long chains). We can summarize the full segmental dynamics of such a binary mixture shown in Figure 2 as (a). This is derived under the condition of $\tau_R > \tau_{obs}$, i.e., $(N_L/N_e)^2 > \gamma$, which is always satisfied in our comparison between theory and experiment in this work. Also depicted in Figure 2 is the behavior (b) of the pure long chain melt. When $\tau_R < \tau_{obs}$, the probe long chain reptates in the bare tube beyond τ_R until τ_{obs} (when short chains move away) before it soon becomes constrained by the other long chains, i.e., confined to the dilated tube. Therefore, $\Phi(t)$ is depicted by lines (c) in Figure 2, where the confinement time can be shown to be given by

$$t_L = (\tau_{obs}/\lambda)(a_L/a)^2 \tag{16b}$$

We once again see that the role of the entangling short chains is twofold: (a) produce tube dilation by constraint release; (b) to impede the diffusion of the long chain in the dilated tube so that the curvilinear diffusion coefficient D is smaller than its Rouse diffusion coefficient D_c.

(ii) Nonentangled Short Chain or Small Molecule Solvent. When the diluent is made of nonentangled short chains or solvent, the description of $\Phi(t)$ follows that for the ideal tube dilation. When the short chain length $N_S \le N_e$, the short chains are expected to speed up the local dynamics of the long chains besides a free volume correction due to lower glass transition temperature of the short chains. In other words, inside the dilated tube, a probe long chain behaves Rouse-like with a higher curvilinear diffusivity $D > D_c$. The mean-square displacement $\Phi(t)$ is simply depicted by the thin lines in Figure 2 as (e), where the disentanglement time is given by eqs 9a−9c with $\lambda < 1$, i.e., $\tau_d < \tau_d^{TD}(N_L,\phi)$ as shown in Figure 2. Also plotted in Figure 2 in dashed lines as (d) is the ideal case where only the effect of tube dilation is present, with $\lambda = 1$.

3. Zero-Shear Viscosity and Terminal Plateau Width. According to the original reptation theory for a monodisperse entangled melt, the plateau modulus G_N^0 is directly related to the entanglement molecular weight M_e and equivalently to the bare tube diameter a. In the simplest cases of entangled solutions and binary mixtures, the suppressed terminal plateau modulus $G_{pl}(\phi)$ implies a relaxed level of entanglement and chain confinement, amounting to the long chains at long times only restricted to a dilated tube of diameter a_L that is related to G_{pl} as depicted in eq 5a. Theoretical speculations of how $G_{pl}(\phi)$ depends on ϕ has been made previously.[31,33]

The zero-shear viscosity η is given by the time integration of the relaxation modulus $G(t)$. For binary mixtures where the short chains' relaxation time is

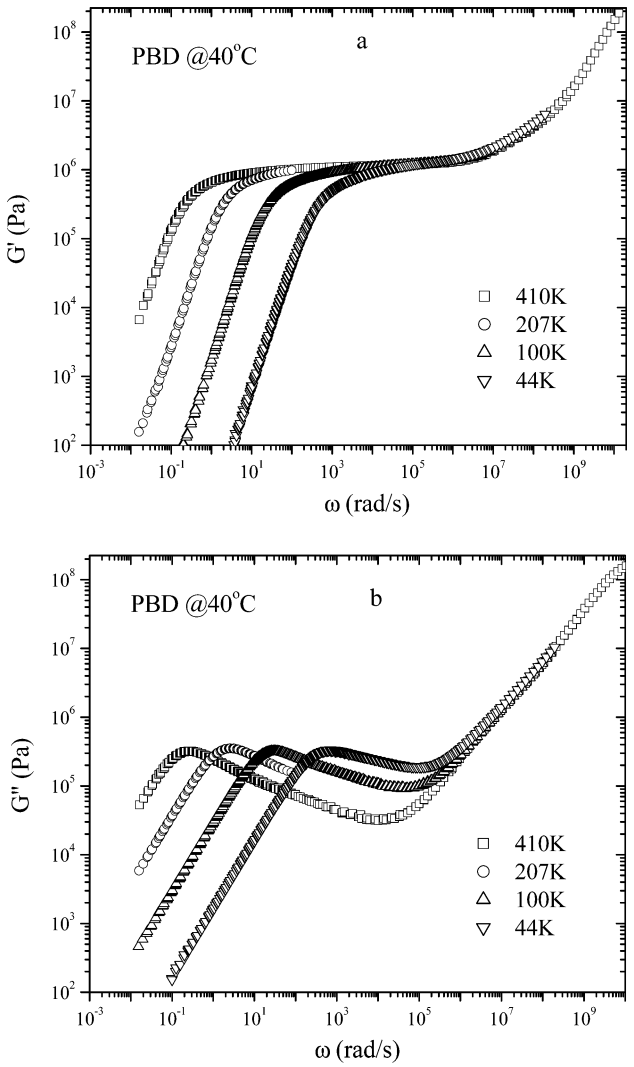

Figure 3. Master curves for (a) G' and (b) G'' of the four high molecular melts.

much smaller and ϕ is not too small, η is approximately given by the product of the terminal plateau modulus and the relaxation time associated with the long chains

$$\eta(\phi) \simeq G_{pl}(\phi)\, \tau_d(N_L,N_S,\phi) \qquad (17)$$

where G_{pl} is given by eq 5a, and τ_d given by eqs 9a−9c, and the additional contribution from the short chains on the order of $G_N^0\, \tau_{d0}^{CLF}(N_S)$ is neglected, a legitimate simplification when the short chains' relaxation time is many orders of magnitude smaller and the long chain's weight fraction is not too low. The decrease of η with lowering weight fraction ϕ of the long chains arises primarily from the depressed plateau modulus and reduced disentanglement time, both due principally to the tube dilation.

It can be shown that the tube dilation characterized by $[a_L(\phi)/a]$ shortens the plateau width of the master curve for the storage modulus G' obtained from oscillatory shear measurements. According to Doi and Edwards,[2] the terminal plateau width measured from G' is given by the ratio (τ_d/t_L) by analogy to that defined for monodisperse melts. Specifically, taking the ratio of the two time scales τ_d and t_L, given by eqs 9a−9c and eq 16a, respectively, and normalizing it with the corresponding ratio for the pure long chain melt, we find

Table 1. Molecular Characteristics of Monodisperse PBD Samples

sample	% 1,4	% 1,2	M_n	M_w	M_w/M_n	T_g (°C)
410K	92.3	7.7	410 800	411 500	1.01	−99.5
207K	91.9	8.1	207 300	207 700	1.01	−100.5
100K	91.8	8.2	98 850	99 060	1.01	−100.1
44K	91.7	8.3	43 450	43 850	1.01	−100.0
12K	91.4	8.6	11 320	11 620	1.03	−100.9
8.9K	91.4	8.6	8 526	8 861	1.04	−102.5
5.8K	91.0	9.0	5 490	5 832	1.06	−102.0
3.9K	90.1	9.9	3 501	3 853	1.10	−101.9
2.0K			1 493	1 991	1.33	

$$\frac{\tau_d/t_L}{\tau_{d0}^{CLF}/\tau_e} = q\left(\frac{a}{a_L}\right)^6 \frac{[1 - X(a_L/a)(N_e/N_L)^{1/2}]^2}{[1 - X(N_e/N_L)^{1/2}]^2} \qquad (18)$$

where $q(N_S,\phi) = \lambda^2/\gamma$ for $N_S > N_e$ and $q = 1$ for $N_S \le N_e$ as shown in Figure 2. Equation 18 shows that the plateau width shrinks relative to that of the pure long chain melt by a factor of approximately $(a_L/a)^6$ due to the tube dilation. The plateau width is separately dependent on the short chain length, i.e., linearly proportional to the parameter $q = \lambda^2/\gamma$. This theoretical prediction can be readily tested experimentally using oscillatory shear measurements to obtain the master curve for G', from which the plateau width (τ_d/t_L) can be evaluated. It is worth mentioning that the VRC theory would predict $q = 1$ independent of N_S because both t_L and T_{rep}^{tube} are proportional to γ in that theory.

4. Critical Concentration for Entanglement. Similar to the case of pure melts where the entanglement vanishes below a particular molecular weight M_e, at which the contour length equals the tube diameter to yield $a^2 = N_e b^2$, there is a particular concentration ϕ_e of long chains below which there are so few long chains that they can no longer confine one another at long times. That condition is supposedly given by setting $L(\phi)$ equal to $a_L(\phi)$ in eq 6

$$[a_L(\phi_e)]^2 = R^2 = N_L b^2 \qquad (19)$$

i.e., $(a/a_L)^2 = N_e/N_L$ at ϕ_e. In other words, when $\phi < \phi_e$ or $a_L(\phi) > R$, the dynamics of long chains are no longer reptative but Rouse-like as described in section II.A.2 for $N_S > N_e$. When $N_S < N_e$, the dynamics are also Rouse-like if hydrodynamic interactions are screened, which is possible[34] when $N_S^2 > N_L$. See Appendix A for a discussion of this case. It is worth noting that the condition depicted by eq 19 is the same as $\beta = (R/a_L)^2 = 1$ used in ref 11. In the present work, we only consider entangled mixtures containing a significant fraction of long chains.

III. Experimental Section

A. Samples. Our model mixtures consist of linear 1,4-polybutadiene (PBD) all synthesized and analyzed in the Goodyear Research Center. Table 1 shows the molecular characteristics of these samples. There are two groups of samples, one of high molecular weights, M_W = 410K, 207K, and 100K, which are termed the "long chains" in this paper, and the other of lower molecular weights, m_w = 44K, 12K, 8.9K, 5.8K, 3.9K, and 2.0K, termed "short chains". The binary mixtures were prepared at the long chain's weight fractions equal to 80%, 60%, 40%, 20%, 10%, and 5%, respectively. Weighed amounts of long and short chain melts were dissolved in toluene over 2−3 days in the dark at room temperature, with periodic manual stirring. After achieving a uniform solution, toluene was then removed under vacuum at room

Table 2. Rheological Parameters for Monodisperse PBD Samples from Oscillatory Shear Measurements

sample	η_0 (Pa s) at 40 °C	a_T (80 °C)	G_c (Pa)	G_N^0 (Pa)	τ_d (s) at 40 °C	η_0/G_c (s) at 40 °C
410K	3.30×10^6	0.264	3.08×10^5	1.15×10^6	4.53	10.7
207K	3.69×10^5	0.261	3.58×10^5	1.15×10^6	0.45	1.03
100K	2.94×10^4	0.254	3.23×10^5	1.18×10^6	0.040	0.091
44K	1.48×10^3	0.241	3.00×10^5	1.20×10^6	0.0019	0.0049
12K	12.7					
8.9K	5.36					
5.8K	1.72					
3.9K	0.7					
2K	0.22					

Table 3. Rheological Parameters for Binary Mixtures

ϕ	η_0 (Pa s) at 40 °C	a_T (80 °C)	G_c (Pa)	$G_{pl}(\phi)$ (Pa)	τ_d (s) at 40 °C	η_0/G_c (s) at 40 °C
			(a) 410K/100K			
0.8	2.06×10^6	0.266	2.04×10^5		4.36	10.1
0.6	1.10×10^6	0.264	1.21×10^5		3.73	9.12
0.4	5.02×10^5	0.269				
0.2	1.67×10^5	0.259				
0.1	7.31×10^4	0.253				
0.05	4.21×10^4	0.254				
			(b) 410K/44K			
0.8	2.08×10^6	0.263	2.14×10^5	6.38×10^5	4.19	9.74
0.6	1.03×10^6	0.264	1.15×10^5	3.28×10^5	3.89	9.02
0.4	3.86×10^5	0.263	4.68×10^4	1.27×10^5	3.42	8.24
0.2	7.07×10^4	0.261	1.13×10^4		2.36	6.28
0.1	1.58×10^4	0.260				
0.05	5.22×10^3	0.256				
			(c) 410K/12K			
0.8	1.88×10^6	0.263	1.94×10^5		4.14	9.69
0.6	9.15×10^5	0.264	1.07×10^5	3.84×10^5	3.63	8.56
0.4	3.33×10^5	0.266	4.39×10^4	1.55×10^5	3.09	7.58
0.2	4.70×10^3	0.259	8.81×10^3	3.00×10^4	2.17	5.34
0.1	5.13×10^3	0.254	1.66×10^3		1.19	3.10
0.05	5.38×10^2	0.244	4.67×10^2		0.37	1.15
			(d) 410K/8.9K			
0.8	1.69×10^6	0.268	1.82×10^5		4.03	9.28
0.6	8.81×10^5	0.267	1.06×10^5	3.90×10^5	3.52	8.30
0.4	3.22×10^5	0.269	4.53×10^4		2.90	7.12
0.2	4.47×10^4	0.259	8.32×10^3	3.06×10^4	1.99	5.37
0.1	4.75×10^3	0.259	1.82×10^3	6.27×10^3	1.03	3.61
0.05	4.76×10^2	0.250	4.70×10^3		0.36	1.01
			(e) 410K/5.8K			
0.8	1.86×10^6	0.268	2.03×10^5		3.96	9.16
0.6	8.17×10^5	0.267	1.02×10^5	3.74×10^5	3.38	7.98
0.4	3.01×10^5	0.269	4.58×10^4		2.72	6.59
0.2	3.26×10^4	0.259	7.96×10^3		1.65	4.10
0.1	3.14×10^3	0.252	1.44×10^3		0.73	2.18
0.05	2.43×10^2	0.246	3.97×10^2		0.21	0.61
			(f) 410K/3.9K			
0.8	1.69×10^6	0.266	1.89×10^5	7.76×10^5	3.83	8.96
0.6	9.14×10^5	0.268	1.17×10^5	4.55×10^5	3.24	7.79
0.4	2.71×10^5	0.266	4.56×10^4	1.73×10^5	2.46	5.95
0.2	2.70×10^4	0.266	7.83×10^3	3.11×10^4	1.32	3.45
0.1	2.50×10^3	0.256	1.76×10^3	7.15×10^3	0.54	1.42
0.05	1.75×10^2	0.247	4.21×10^2		0.14	0.41
			(g) 410K/2.0K			
0.8	1.71×10^6	0.271	2.07×10^5	7.51×10^5	3.53	8.25
0.6	6.95×10^5	0.273	1.08×10^5	4.49×10^5	2.70	6.41
0.4	2.15×10^5	0.274	4.72×10^4	1.88×10^5	1.84	4.55
0.2	2.43×10^4	0.272	1.04×10^4	4.33×10^4	0.89	2.33
0.1	2.41×10^3	0.268	2.39×10^3	1.11×10^4	0.35	1.01
0.05	1.77×10^2	0.245	5.95×10^2		0.09	0.30
			(h) 207K/12K			
0.8	1.72×10^5	0.260	1.78×10^5		0.41	1.03
0.6	8.27×10^4	0.261	9.88×10^4	2.87×10^5	0.35	0.97
0.4	3.03×10^4	0.258	4.27×10^4	1.28×10^5	0.29	0.84
0.2	4.46×10^3	0.248	8.41×10^3	2.69×10^4	0.17	0.71
0.1	5.15×10^2	0.242	2.56×10^3		0.066	0.53
0.05	98.3	0.243				
			(i) 100K/12K			
0.8	1.69×10^4	0.259	2.09×10^5		0.034	0.080
0.6	7.30×10^3	0.258	1.09×10^5		0.029	0.067
0.4	2.24×10^3	0.256	4.33×10^4		0.021	0.052
0.2	3.69×10^2	0.250	1.41×10^4		0.0083	0.026
0.1	77.6	0.241				
0.05	35.1	0.214				

temperature for at least 1 week until the sample had less than 0.2% of toluene.

B. Apparatus. Linear viscoelastic properties of the PBD mixtures are measured by a dynamic mechanical spectrometer

(Advanced Rheometrics Expansion System-ARES) at frequencies ranging from 0.1 to 100 rad/s and temperatures from 100 to −80 °C. The spectrometer is equipped with a 200−2000 g cm dual range and force rebalance transducer, and oscillatory shear measurements are carried out using a 25 or 8 mm diameter parallel plate flow cell.

Dynamic shear experiments are carried out to measure the storage and loss moduli G' and G'' of the monodisperse samples and binary mixtures made of monodisperse high molecular weight and low molecular weight 1,4-polybutadienes. Several important rheological properties can be evaluated from the master curves for G' and G'', including the zero-shear viscosity η_0, plateau modulus G_N^0 or $G_{pl}(\phi)$, plateau width, and terminal relaxation time, i.e., disentanglement relaxation time τ_d.

IV. Results

As the baselines, we first present the master curves for the storage and loss moduli in parts a and b of Figure 3, respectively, from oscillatory shear measurements of 410K, 207K, 100K, and 44K monodisperse samples. The key characteristics from these measurements are listed in Table 2, where the shift factor is against the reference temperature at 40 °C, the modulus G_c at the crossing point is defined as $G_c = G'(\omega_c) = G''(\omega_c) \cong G''_{max}$, and the plateau modulus G_N^0 is the value of $G'(\omega_{min})$ where $G''(\omega_{min})$ attains a minimum at ω_{min}. Also tabulated are the zero-frequency viscosity values of other lower molecular weight melts, which show in Figure 17 that the oligomers of 3.9K and 2K are below the entanglement and 5.8K is only slightly entangled.

The effects of blending short chains into a melt of long chains are severalfold: depressing the terminal modulus, modifying the terminal relaxation time, and thus reducing the zero-shear viscosity. The dynamics of short chains are also affected by the surrounding long chains. As an example, Figure 4a,b shows G' and G'' for binary mixtures of 410K and 100K. Also presented is G'' in linear scale as shown in Figure 4c, which resembles Figure 9 in ref 28 and Figure 1b reported by Rubinstein and Colby:[35] the terminal peak positions hardly shift with dilution. This has been taken previously as evidence that the long chains undergo pure reptation in the bare tube.[28]

According to the theoretical treatment presented in the previous section, tube dilation (TD) occurs because short chains relax much faster than the long chains. In other words, the terminal plateau modulus associated with TD may be manifested in a universal way *independent of* short chain length N_S. Figure 5a shows the storage modulus G' of binary mixtures at a concentration $\phi = 0.6$, i.e., 60 wt % of the long chain with 40 wt % of short chains, where the long chain has a molecular weight of 410K and the different short chain matrices are of molecular weights m_w = 100K, 44K, 12K, 8.9K, 5.8K, 3.9K, and 2.0K. Within the experimental uncertainty of ±10%, a common plateau modulus $G_{pl}(\phi)$ can indeed be identified for all the different short chain lengths. Moreover, the terminal plateau width, which can be quantified by the ratio of τ_d to t_L, varies strongly with the short chain length, suggesting that the parameter q in eq 18 is a sharply decreasing function of N_S. For completeness, G'' is also plotted for these mixtures as shown in Figure 5b. The constant WLF shift factor a_T shown in Figure 5c for this series indicate that there is no difference among these samples in terms of any variation of the glass transition temperature with the short chain length. The independence of $G_{pl}(\phi)$ on N_S and its dependence on ϕ can be further illustrated in Figure 5d involving two other mixtures at three concentrations.

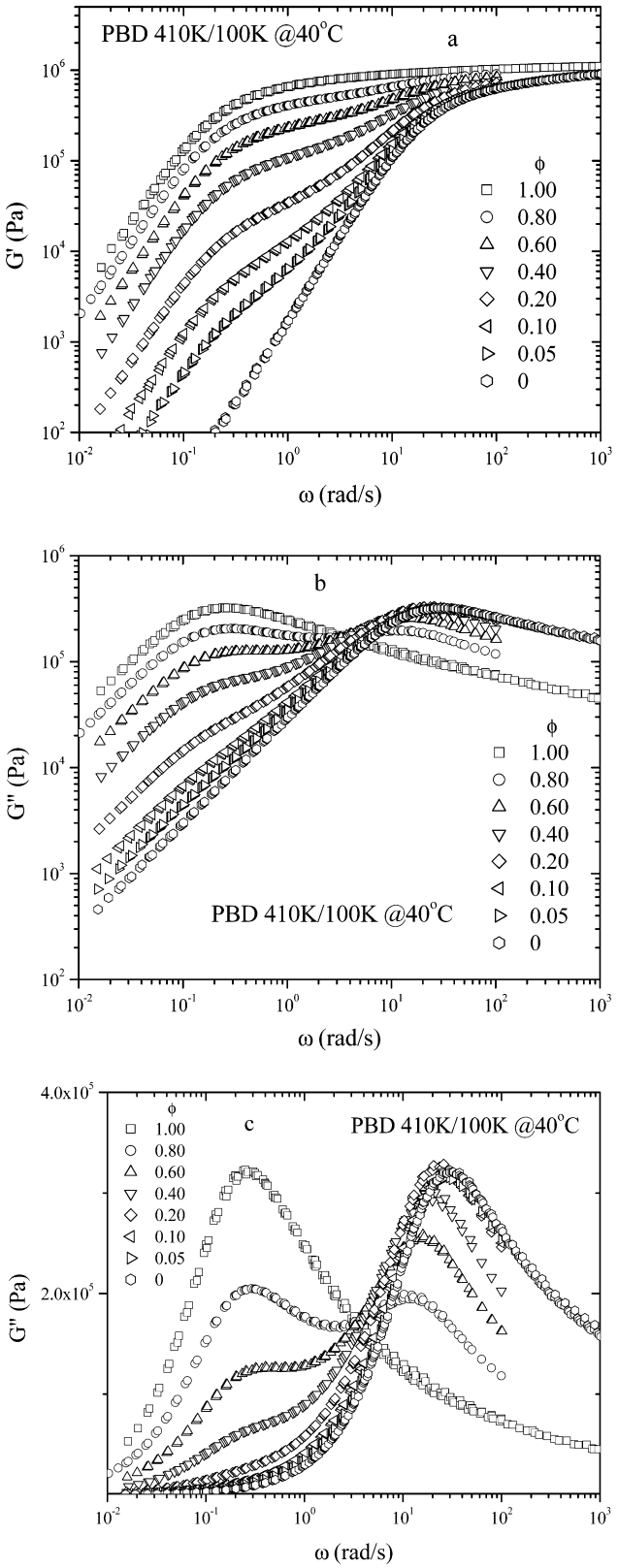

Figure 4. Master curves for (a) G' and (b) G'' of the binary mixtures involving 410K and 100K. (c) G'' on a linear scale to highlight the twin peak characteristics.

The effect of blending short chains in a long chain melt can be further demonstrated in terms of the terminal behavior in the 410K/44K mixtures as shown in Figure 6a,b. Although difficult to notice, the peak

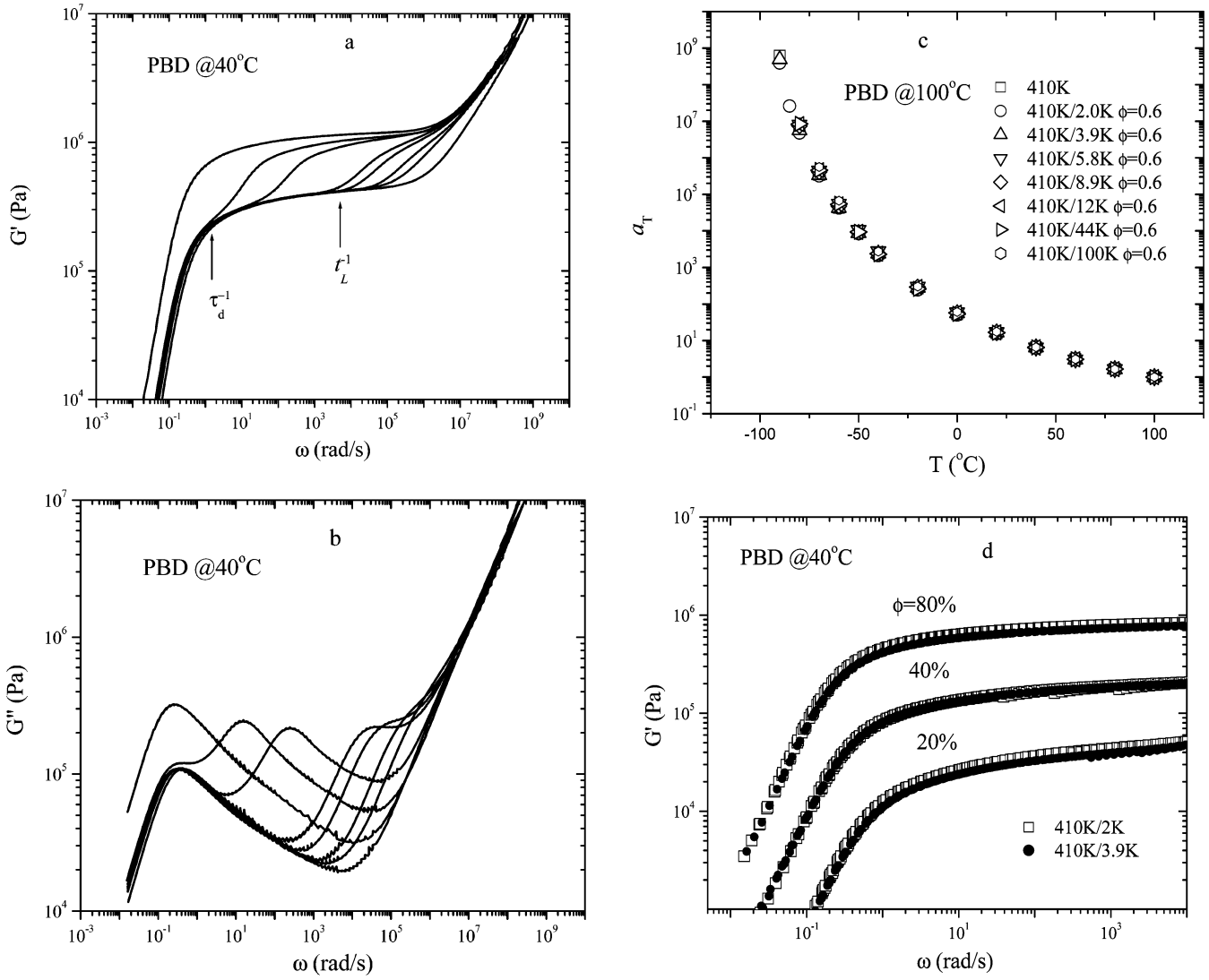

Figure 5. (a) Master curves of G' for the pure 410K melt as well as its binary mixtures at $\phi = 0.6$ with different lower molecular weight components (from the left to the right-hand side): 100K, 44K, 12K, 8.9K, 5.8K, 3.9K, and 2.0K, where a small amount of vertical shift (<±10%) was made to line up to the same G_c to remove the loading inaccuracy. Since the meaning of G_c is doubtful for 410K/100K, that particular curve was vertically shifted slightly to achieve overlap with the others in the Rouse regime. The approximate locations of the reciprocal terminal relaxation time τ_d and the tube confinement time t_L of eq 16a for 410K/12K are also respectively indicated. (b) Master curves of G'' for the same samples as described in (a). (c) The WLF shift factors corresponding to the pure 410K and its mixtures depicted in (a) and (b), where the reference temperature is 100 °C. At 40 °C where we evaluate the relaxation times for this and other series below, the values of a_T are as follows: 410K: 6.57; 410K/100K: 6.58; 410K/44K: 6.53; 410K/12K: 6.54; 410K/8.9K: 6.60; 410K/5.8K: 6.50; 410K/3.9K: 6.51; 410K/2.0K: 6.25. (d) G' at three concentrations $\phi =$ 0.8, 0.40, and 0.2 of binary mixtures involving 410K/3.9K and 410K/2.0K.

position of G'' actually shifts to the right with decreasing ϕ, along with the decreasing plateau modulus. The terminal chain dynamics are shifted more significantly in the mixtures of 410K/3.9K, as shown in Figure 6c,d. Finally, the master curves for the 410K/2K mixtures show in Figure 6e the characteristics typical of highly concentrated solutions where both vertical and horizontal shifts have been made to achieve overlap in the terminal region. Unlike other blends, the short chains of 2K are not entangled as can be seen from the molecular weight dependence of viscosity in Figure 17. Therefore, we hardly see any shoulder in G'' in comparison to Figure 6d.

We would like to obtain $G_{pl}(\phi)$ as a function of ϕ for all short chain lengths. For this purpose it is not necessary to acquire all the master curves at different concentrations. Instead, we can generalize the well-known relation[28,36] between G_N^0 and G''_{max} of $G_{pl} \simeq 3.56G''_{max} = G_c$, where $G_c \equiv G'(\omega_c) = G''(\omega_c)$. For mixtures for which we have partial master curves to obtain G_{pl} as the value of $G'(\omega_{min})$ at ω_{min} where $G''(\omega_{min})$ is at its minimum, we have confirmed this empirical relation as shown in Figure 7a, where the two lines are vertically separated by 3.56. The relevant rheological parameters such as the zero-frequency viscosity η_0 and disentanglement time $\tau_d = 1/\omega_c$ have been evaluated from such oscillatory shear measurements and are listed in Table 3 for several families of binary mixtures.

The variation of tube dilation (TD) with the weight fraction ϕ can be systematically evaluated according to eq 5a using $G_{pl} \propto G_c$. Plotted in Figure 7b is ϕ dependence of the dilated tube diameter calculated from Figure 7a using eq 5a. The observed scaling indicates that TD is independent of the short chain length at all the concentrations and agrees with the previous findings.[22,28] At low concentrations, the determination of G_c becomes less accurate.

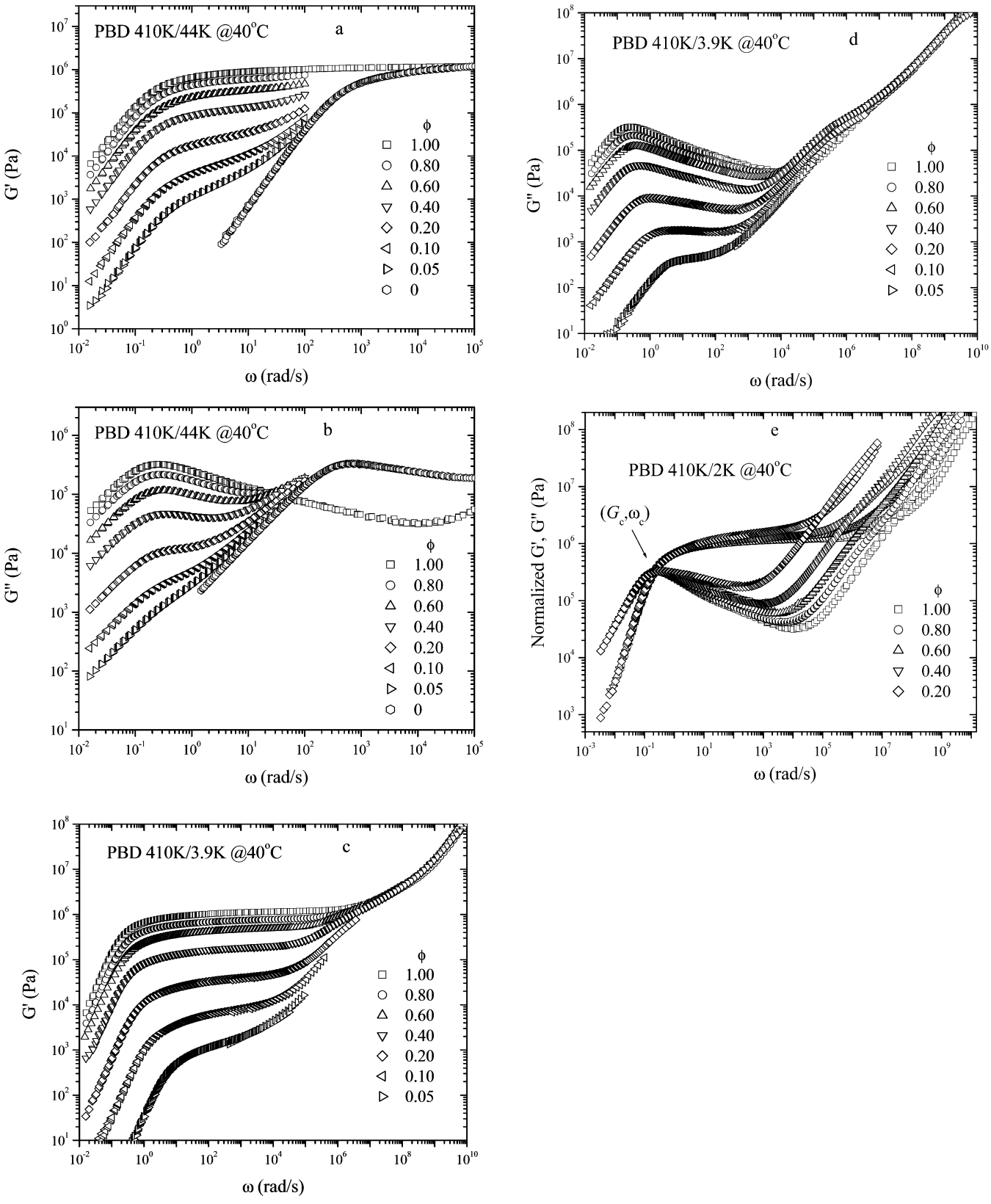

Figure 6. Master curves for (a) G' and (b) G'' of the 410K/44K mixtures including those for the pure 410K and 44 melts. Master curves for (c) G' and (d) G'' of the 410K/3.9K mixtures including those for the pure 410K melt. (e) Master curves for G' and G'' of the 410K/2.0K mixtures including those for the pure 410K melt, shifted to coincide at the crossing point (G_c, ω_c).

In the present work, we are interested in understanding how short chains of different lengths affect the terminal relaxation behavior of the long chains in the binary mixtures. The terminal relaxation time τ_d can be approximately obtained either through a measurement of the zero-shear viscosity η_0 in conjunction with the terminal plateau modulus G_{pl} according to eq 17 or by determining the crossing point of the storage and loss moduli G' and G'' where $G'(\omega_c) = G''(\omega_c)$ and identifying $\tau_d = 1/\omega_c$. The zero-frequency viscosity η_0 can be

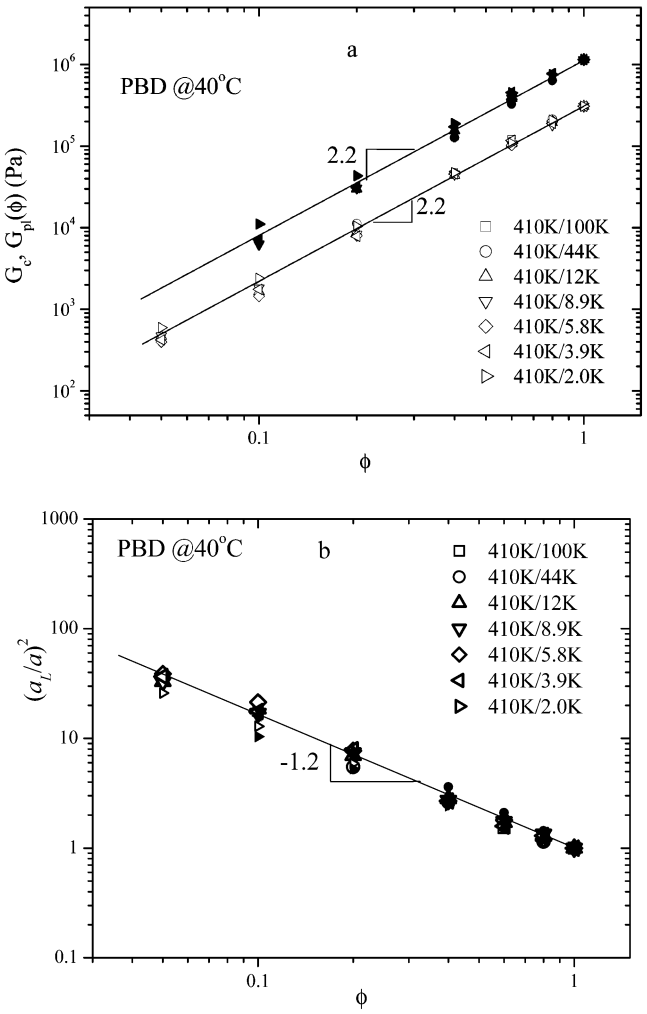

Figure 7. (a) Terminal plateau modulus $G_{pl}(\phi)$ and crossing modulus G_c of different binary mixtures in filled and open symbols, respectively. (b) Normalized diameter (a_L/a) of the dilated tube calculated from (a) according to eq 5a.

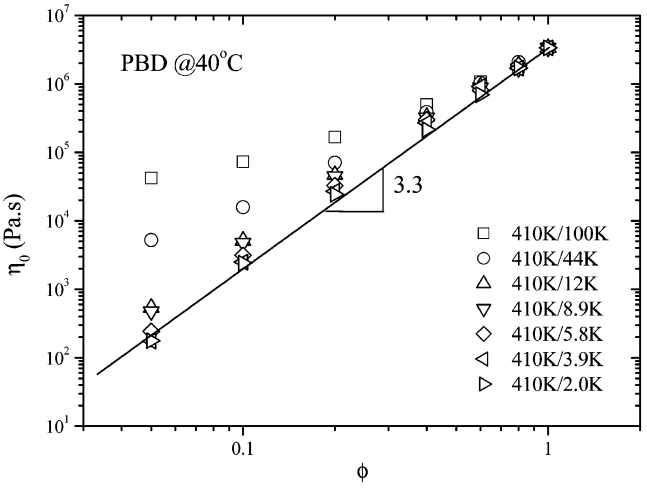

Figure 8. Zero-frequency viscosity η_0 as a function of concentration for the different binary mixtures as indicated.

measured from oscillatory shear measurements of G' and G'' in the low-frequency limit of $\sqrt{G'^2+G''^2}/\omega$. Figure 8 shows η_0 as a function of concentration ϕ for different short chain lengths. The effect of entangled short chains on the concentration dependence of η_0 is rather evident. In the limit of $m_w = 2.0$K, the scaling

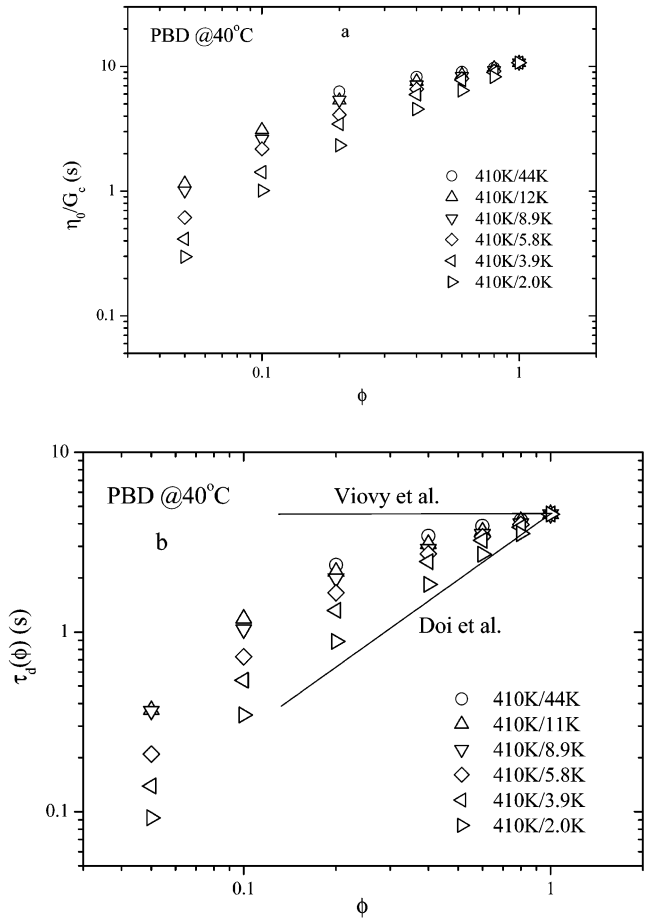

Figure 9. (a) Terminal relaxation time estimated from η_0 and G_c for the different binary mixtures. (b) The disentanglement time τ_d taken from the crossing frequency: $\tau_d = 1/\omega_c$ at which $G'(\omega_c) = G''(\omega_c)$, where the horizontal and inclined lines represent the predictions by the previous theories.

exponent is 3.3, comparable to previous findings of concentrated polymer solutions[37−40] and to the prediction based on eq 17 for the scaling of η_0 with ϕ, which is $\phi(a/a_L)^4$ assuming λ is close to unity. At sufficiently low ϕ and for 410K/100K and 410K/44K, the scaling law no longer holds because of the short chains' contributions.

Figure 9a,b shows respectively the numerical values of η_0/G_c and of τ_d as a function of concentration ϕ for short chains of different molecular weights. Here Figure 9a is obtained from a combination of Figures 7a and 8, and Figure 9b is obtained from the terminal behavior of G' and G''. Namely, $\tau_d = 1/\omega_c$, where $G'(\omega_c) = G''(\omega_c)$. According to eq 7.47 of ref 2, $\eta_0/G_{pl} = (\pi^2/12)\tau_d$; thus, $\eta_0/G_c = 3.56(\pi^2/12)\tau_d \simeq 2.9\tau_d$. Indeed, there is a difference of more than two between parts a and b of Figure 9.

The concentration dependence of the terminal dynamics can be also illustrated based on the oscillatory shear measurements in terms of the calculated relaxation modulus $G(t)$. Figure 10a shows $G(t)$ for several concentrations for mixtures of 410K/44K. In contrast, Figure 10b shows a larger concentration dependence for the mixtures of 410K/3.9K, consistent with the trends shown in Figure 9b. We can also compare the dependence of the relaxation behavior on the short chain length as shown in Figure 10c for 410K in different short chains at the weight fraction of $\phi = 0.6$. To make them distinguishable, only 410K/100K, 410K/12K, 410K/5.8K, and 410K/2K data are shown in Figure 10c to compare with 410K pure melt data. All the conversions

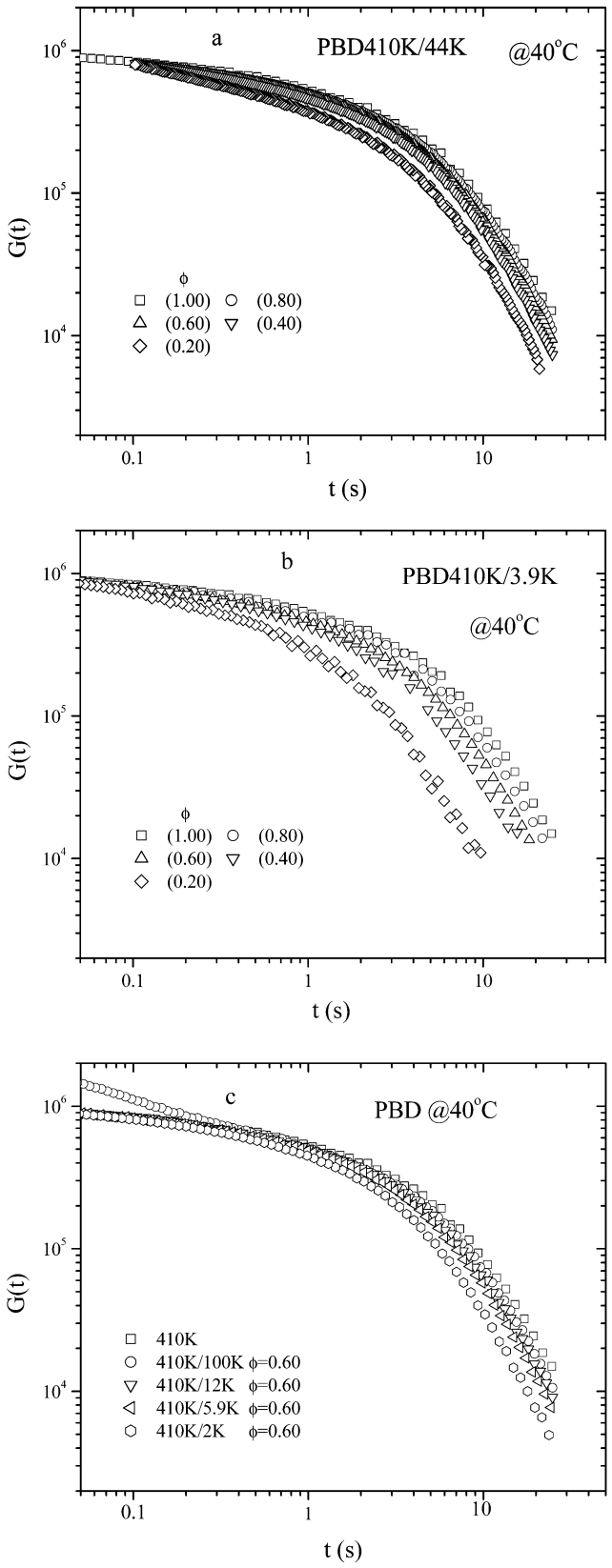

Figure 10. (a) Relaxation modulus $G(t)$ for the 410K/44K mixtures, calculated from Figure 6a,b after shifting to a common G_c. (b) The relaxation modulus $G(t)$ for the 410K/3.9K mixtures, calculated from Figure 6c,d after shifting to a common G_c. (c) The relaxation modulus $G(t)$ for the pure 410K and its seven binary mixtures at $\phi = 0.6$ with 100K, 12K, 5.8K, and 2K, calculated from Figure 5a,b after shifting to a common G_c.

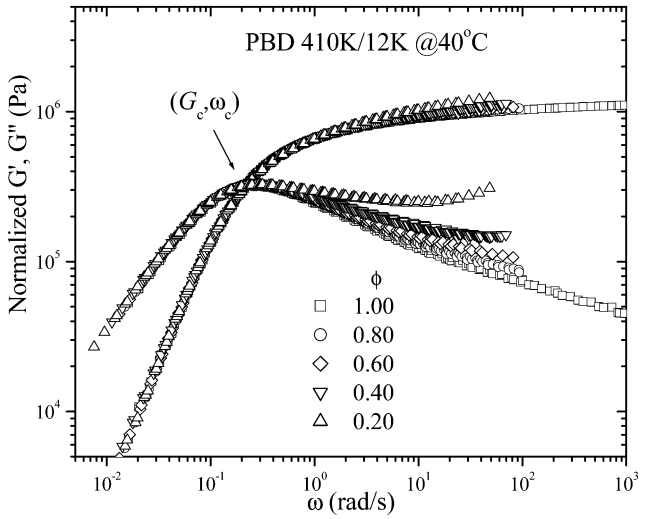

Figure 11. Terminal characteristics of the 410K/12K mixtures at different concentrations, shifted to coincide at the crossing point (G_c, ω_c).

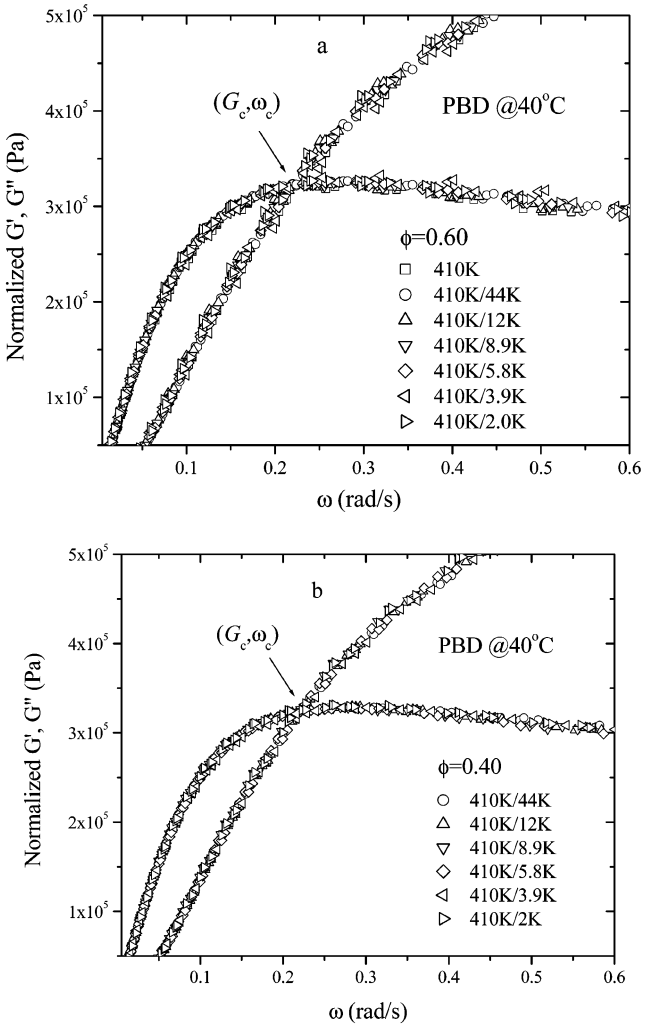

Figure 12. Terminal characteristics of the different mixtures at concentrations (a) $\phi = 0.6$ and (b) $\phi = 0.4$, both shifted to coincide at the crossing point (G_c, ω_c).

from G' and G'' to $G(t)$ employ a procedure given within the ARES that is based on the method outlined in eq 48 in Chapter 4 of ref 24.

It may be necessary to show that the physical meaning of the crossing frequency ω_c at $G'(\omega_c) = G''(\omega_c)$ as an estimate of the reciprocal disentanglement time has not changed from a monodisperse melt to binary mix-

tures involving respectively a particular short chain length at different concentrations and a particular concentration with different short chain lengths. Figure 11 shows, after both vertical and horizontal shift to bring the crossing point together, that the terminal characteristics for the 410K/12K mixtures, i.e., the shapes of G' and G'', remain identical at low frequencies up to the crossing point at all concentrations. On the other hand, we can also compare G' and G'' for different short chains as shown in Figure 12a,b at two concentrations. We see that the master curves are identical around the crossing point for all short chain lengths.

We have also examined how the same short chains affect the terminal dynamics for long chains of different molecular weights. Figure 13a shows the normalized disentanglement times as a function of ϕ for long chains of molecular weights $M_W = 410K$, 207K, and 100K in a matrix of uniform short chain length with $m_w = 12K$, where the symbols are the experimental data and the dashed lines are predictions that include the effect of the enhanced contour length fluctuation. Further discussion on this figure follows in the next section. The nearly identical WLF shift factor in Figure 13b indicates that the variation of the disentanglement time with ϕ is not due to any difference in the dynamics due to a variation of the glass transition temperature with ϕ.

V. Data Analysis and Discussion

A. Effect of Contour Length Fluctuation. Since the impedance function λ of eq 9c in eq 9a is by definition independent of N_L and the tube dilation is only a function of ϕ, the data splitting among the different long chain lengths in Figure 13a requires an explanation. To our knowledge, it is the first time when the measurements are carried out with such accuracy that we can demonstrate the difference in the concentration dependence for the different molecular weights as shown in Figure 13a. Here we suggest that the split arises from the effect of contour length fluctuation (CLF). To our knowledge, this is the first time that CLF is visualized and shown to be enhanced due to the tube dilation as depicted in eq 8, relative to that of eq 2a for monodisperse melts. The CLF effect is stronger for a lower molecular weight sample and also increases with increasing tube dilation (i.e., lowering ϕ) according to eq 8 or eqs 9a and 9b. Thus, at a lower concentration, the influence of the CLF effect on the disentanglement time is greater. At any concentration, the difference in the normalized relaxation times between two long chain lengths can be written in terms of the ratio of the normalized times, for example, 410K to 100K, as

$$\frac{(\tau_d/\tau_{d0}^{CLF})_{100K}}{(\tau_d/\tau_{d0}^{CLF})_{410K}} = \frac{[1 - X(a_L/R_{100K})]^2[1 - X(a/R_{410K})]^2}{[1 - X(a_L/R_{410K})]^2[1 - X(a/R_{100K})]^2} \quad (20)$$

where R_{410K} and R_{100K} are the mean chain end-to-end distances for the chains of molecular weights 410K and 100K, respectively. Taking X to be 1.45, we describe how much splitting is expected using the experimental data for 410K as the baseline. The theoretical account as shown in Figure 13a with the dashed lines agrees satisfactorily with the actual experimental data. This work appears to be the first to elucidate the CLF effect

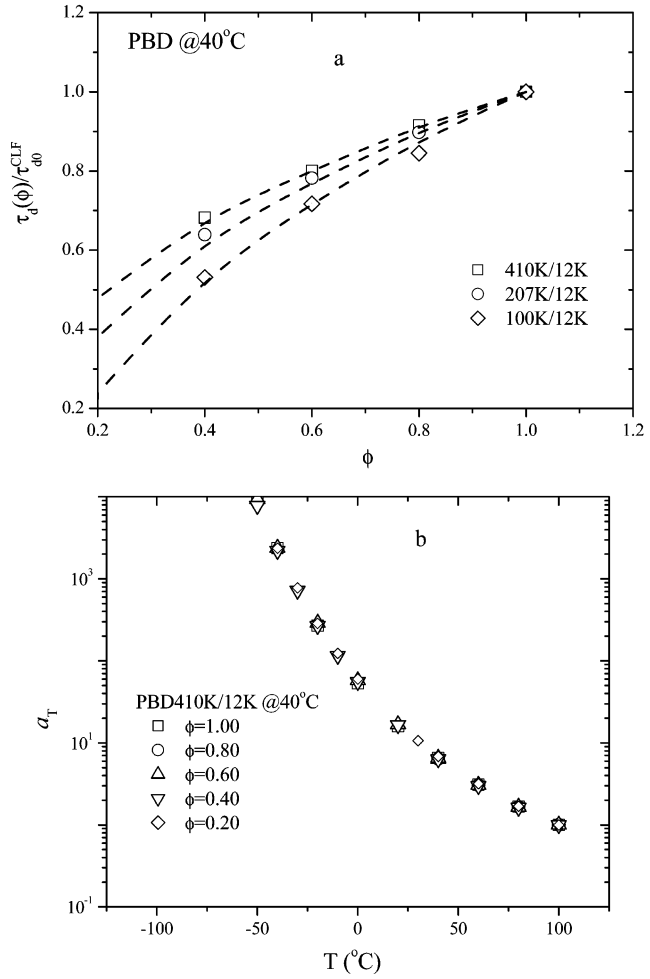

Figure 13. (a) Normalized terminal relaxation time τ_d/τ_{d0}^{CLF} as a function of concentration in binary mixtures involving long chains of three different molecular weights $M_W = 410K$, 207K, and 100K in the same short chains of molecular weight $m_w = 12K$. (b) The WLF shift factor a_T at different weight fractions of 410K in 12K. At 40 °C where we evaluate the relaxation times for this series, the values of a_T are as follows: $\phi = 1.0$: 6.6; $\phi = 0.8$: 6.4; $\phi = 0.6$: 6.5; $\phi = 0.4$: 6.3; $\phi = 0.2$: 6.8.

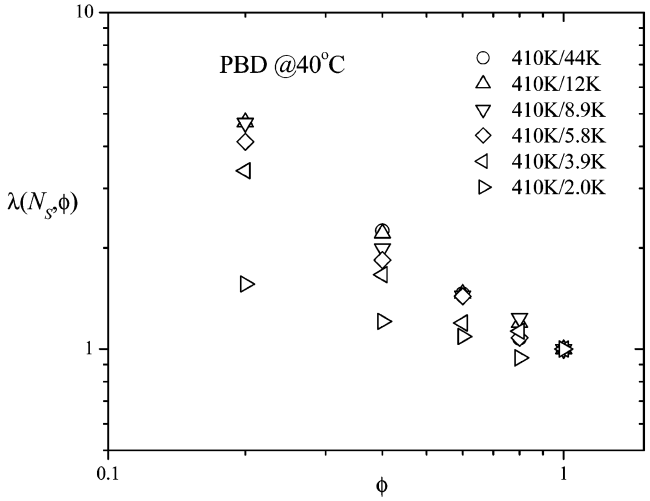

Figure 14. Impedance function λ evaluated according to eq 21 from the experimental data in Figure 7b for the tube dilation and Figure 9b for the disentanglement times $\tau_d(\phi)$ and $\tau_{d0}^{CLF} = \tau_d(\phi=1)$.

through the concentration dependence of the terminal relaxation times for various molecular weights. It is

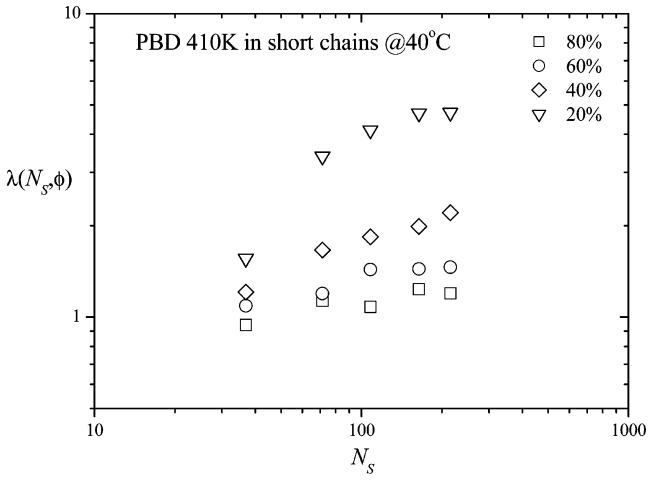

Figure 15. Impedance function λ as a function of N_S at four concentrations calculated from Figure 14.

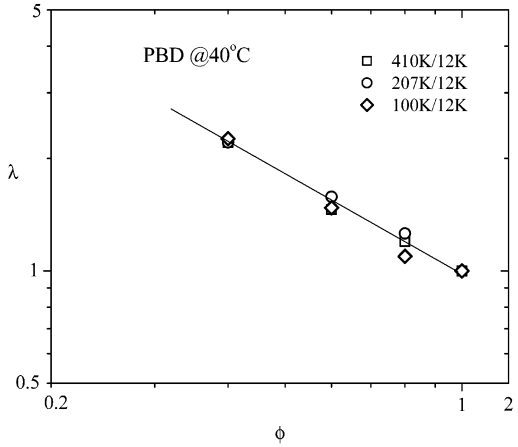

Figure 16. Impedance function λ evaluated according to eq 21 from the experimental data in Figure 13a.

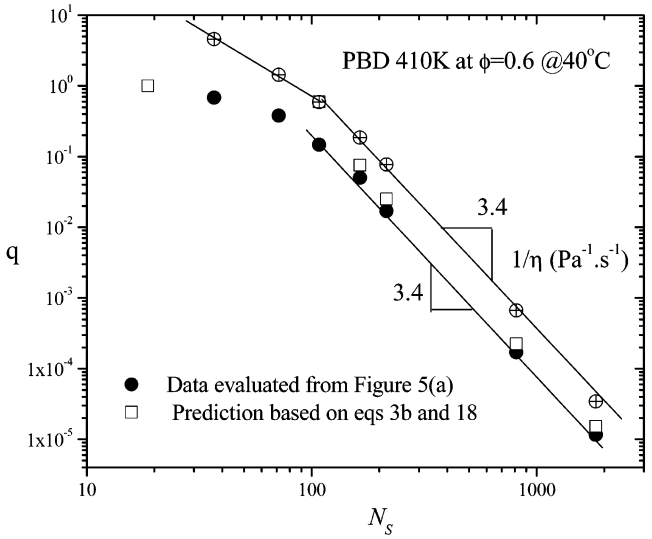

Figure 17. The parameter q in eq 18, experimentally estimated from Figure 5a (in circles) and predicted according to $q = \lambda^2/\gamma$ using eq 3c without the CR factor (in squares) and experimental values of λ from Figure 14, and the measured zero-shear viscosity η_0 as a function of the short chain length N_S.

worth noting that the larger CLF corrections at finite concentrations results in a scaling exponent for the scaling of the terminal relaxation time with the molecular weight that is not constant and instead dependent on ϕ. The successful theoretical account for split in Figure 13a offers supporting evidence that the tube dilation is present to enhance the CLF correction in these mixtures. Since $1 < \alpha(N_L,N_S) = 6.8$ and 3.3 for 100K/12K and 207/12K, respectively, the tube dilation as visualized here is not anticipated by the previous theories.

B. Unknown Curvilinear Diffusivity *D* or Impedance Function λ. Our data for 410K/44K and 100K/12K both satisfy the condition of $N_L N_e^2/N_S^3 \ll 1$ or $\alpha \gg 1$ in eq 4b. According to Struglinski and Graessley[28] and to the theories of Viovy et al.[11] and Doi et al.,[23] the long chain's disentanglement time should equate that of the pure long chain melt. However, Figure 9a,b shows that the terminal relaxation time in the binary mixtures is always smaller than that of the pure 410K. Moreover, the long chain disentanglement times depend explicitly on the short chain length and on the weight fraction ϕ.

According to the previous theory of Doi et al. presented in section II.B.1, the terminal relaxation time for mixtures with $\alpha \leq 1$ should be depicted by eq 9b, i.e., its concentration dependence being independent of the short chain length in contradiction to the experimental data in Figure 9b. On the other hand, in the theory of Viovy et al. in section II.B.2, the terminal dynamics of the long chains in these mixtures of 410K with 12K, 8.9K, and 5.8K are expected to be unaffected by the incorporation of these short chains because the parameter γ of eq 3c (without the CR factor) is 122, 34, and 4, respectively, leading to $(a/a_L)^2\gamma(N_S) > 1$ in eq 7 throughout the composition range for these mixtures. In other words, the terminal relaxation time is expected to be independent of ϕ and equal to that of the pure long chain melt. This is also in explicit contradiction with the experimental data in Figure 9b. In highlight, for mixtures 410K/12K, 410K/8.9K, and 410K/5.8K, the previous theories only provide the bounds within which the experimental data exist as shown in Figure 9b.

As discussed in the previous subsection, the CLF correction is greater in the presence of the tube dilation according to eq 8. In other words, with decreasing ϕ the disentanglement process involves an increased CLF correction that lowers the relaxation time, contributing partially to the observed decrease observed in Figure 9a,b. However, there is no theoretical basis to assert that this enhanced CLF effect should depend on the short chain length when $\tau_R \gg \tau_{obs}$, i.e., $(N_L/N_e)^2 \gg (N_S/N_e)^3$. Thus, we are confronted with the challenge to explain why the concentration dependence of τ_d varies systematically with the short chain's molecular weight.

Our new theoretical analysis given in eqs 9a−9c offers a plausible explanation of the experimental data because the impedance parameter λ in eqs 9a and 9c can account for the additional dependence on ϕ and N_S. In the dilute long chain limit, a long chain's diffusion on the length scale of $R = \sqrt{N_L}b$ in a matrix of short chains may indeed be depicted by the constraint-release diffusion constant D^{CR} of eq 4a. At a finite concentration of long chains in a matrix of short chains, a probe long chain not only finds its motion confined at short times by both short and long chains as depicted in Figure 1a but at long times (when short chains disentangle) by other long chains as shown in Figure 1b. The curvilinear diffusive movement of a long chain in the dilate tube depends on the coupling between the terminal short chain dynamics and local long chain dynamics. This

dynamic coupling varies with the length scales set by the diameter $a_L(\phi)$ of the dilated tube and with N_S. In this dilated tube only a fraction of short chains (that are involved in the dilute limit to produce D^{CR}) are available to interfere with the curvilinear motion of the probe long chain. Thus, D in eq 9a that depicts this movement also depends on the concentration ϕ. In other words, λ in eq 9a is not simply a constant equal to γ independent of ϕ as proposed by Viovy et al.;[11] instead, it depends explicitly on ϕ and N_S in some nontrivial way.

An explicit derivation of the impedance function $\lambda(N_S,\phi)$ is currently unavailable. This many-body problem cannot be reliably treated with a scaling argument, and no straightforward mean-field approach has been established. The emergence of this impedance function within a reptation model framework arises from the employment of the coarse-grained picture depicted in Figure 2b, which recognizes the importance of tube dilation that occurs when short and long chain's relaxation times are separated by many decades. Although it is beyond the scope of this work to explore any theory that predicts λ as a function of N_S and ϕ, λ is expected in our coarse-grained model to be an increasing function of N_S and a decreasing function of ϕ. *Within* the reptation model, we can proceed to determine λ by comparing the theoretical result of eqs 9a−c with the experimental data in Figure 9b since all the other factors can be reliably obtained from experiment. In particular, the data in Figure 9b can be divided by the relaxation time $\tau_{d0}^{CLF} = 4.5$ s of the 410K pure melt to yield the normalized disentanglement time τ_d/τ_{d0}^{CLF}, in terms of which λ in eq 9a has the following expression:

$$\lambda(N_S,\phi) = [\tau_d(N_L,N_S,\phi)/\tau_{d0}^{CLF}(N_L)](a_L/a)^2 \frac{[1 - X(N_e/N)^{1/2}]^2}{[1 - X(a_L/a)(N_e/N)^{1/2}]^2} \quad (21)$$

where the tube dilation factor (a_L/a) can be estimated from the measurement of the plateau modulus as shown in Figure 7b, $N_e/N_L = M_e/M_W$ is known with $M_e = 1.5$K from Fetters et al.,[41] and X is taken as 1.45 according to Doi.[2,3] Thus, a combination of the two data sets from Figure 9b and Figure 7b allows us to extract the impedance function λ as shown in Figure 14 as a function of ϕ for different short chain molecular weights.

Figure 15 indicates that the N_S dependence of λ is stronger at lower concentrations. Below the critical concentration for entanglement, i.e., for $\phi < \phi_e$ where $a_L(\phi) > R$, the chain diffusivity might be given by eq 4a. For the concentrations studied here, the long chains are entangled among themselves, and λ's dependence on N_S is rather weak. With increasing concentration, there are fewer short chains penetrating into the dilated tube to hinder the curvilinear diffusion of the long chain. Consequently, λ stays close to unity and increases only weakly with N_S. Conversely, at lower concentration many more short chains participate in entanglement with the probe long chain, causing more significant slowing down of the curvilinear diffusion. This is clearly demonstrated in Figure 15.

Similarly, we can evaluate λ from Figure 13a according to eq 21 where the tube dilation is taken to obey the scaling law given in Figure 7b. Figure 16 displays a master curve to indicate that λ is indeed insensitive to the long chain length as expected from its definition in eq 9c.

C. Plateau Width. Finally, we test our theoretical prediction of eq 18 against the experimental observation. Experimentally, we can determine the parameter q in eq 18 by first measuring the plateau widths from Figure 5a for both the mixtures and the pure long chain melt to get the ratio on the left-hand side of eq 18. The right-hand side of eq 18 essentially involves the tube dilation factor that can be obtained from Figure 7b. Therefore, the value of q can be experimentally determined as a function of N_S, as shown in Figure 17. Theoretically, q can be evaluated according to $q = \lambda^2/\gamma$, where the value of λ is experimentally known from Figure 14 and γ can be computed from eq 3c without the CR factor. At the finite weight fractions of the long chains, a considerable amount of obstacles are the long chains; thus, the CR effect becomes negligible. The comparison between the data and prediction is rather impressive as q varies nearly 5 orders of magnitude. This comparison is interesting and approximately validates the detailed structure of the model. In other words, besides the key feature of the theory depicted in Figure 14 for the impedance function λ inferred from a comparison with the experiment, eq 18 describes the short time dynamics of the theory, predicting the parameter q to have specific dependence on the short chain length at different concentrations in good agreement with the measurements.

VI. Conclusion

We have carried out a systematic experimental study to elucidate the terminal relaxation behavior of entangled binary mixtures of long and short chains. The extensive data, available for the first time, have inspired the development of a new reptation theory for such mixtures. We have shown both experimentally and theoretically how the short chains, when blended with long chains of the same species, affect the long chain's dynamics at different time scales by (a) dilating the tube that confines the long chain to only move longitudinally along its primitive path before the disentanglement time and (b) impeding the curvilinear diffusion of the probe chain within the dilated tube. Specifically, a new phenomenological reptation model is proposed to depict this dual effect of the short chains and to compare with the experimental observation.

The reptation theory presented in this paper deviates substantially from the previous reptation models.[11,23] It was argued in ref 11 that the long probe chain would remain confined in the bare skinny tube for $N_S > N_e$, and only the *bare tube* would move in the dilated tube (so-called supertube) as depicted by eq 7 for $\alpha < 1$. In ref 23, it was argued that whenever α of 4b is smaller than ϕ, the terminal relaxation time would be τ_d^{TD} of eq 9b, which is independent of the short chain length N_S. These theoretical predictions are found to explicitly disagree with the present experimental data. In our theory we envision that the probe long chain experiences a coarse-grained environment defined by the dilated tube where frictional drag on the reptating long chain depends on the tube diameter a_L, i.e., ϕ, and on the short chain length N_S. The new model is built on the plausible notion of tube dilation, as depicted in Figure 1b and quantified by the factor (a_L/a), which can occur for binary mixtures as long as the short chain disentangles much faster than the long chain and is a major constraint release process that allows the probe chain (not the bare tube, as visualized in Viovy et al.[11]) to

reptate out the dilated tube over a shorter contour length $L(\phi) < L$ given in eq 6. Whether and how much the tube dilation shortens the long chain's reptation time depends on the second factor, i.e., on how the short chains impede curvilinear diffusion within the dilated tube. This second factor has been overestimated previously in ref 11 using the original constrain release ideas[25−27] and assumed to be independent of the short chain length in ref 23.

It appears that our new theory has the correct basic ingredients to evaluate the influence of short chains on the long chain dynamics for linear polymer mixtures. The three basic ingredients are (1) enhanced contour length fluctuation, (2) tube dilation, and (3) impedance of curvilinear diffusion. A fourth factor, i.e., (4) constraint release, is negligible for our current systems but can become appreciable when the long chains' molecular weight and weight fraction are lower than considered in the present work. We hope to extend the theory to describe time-dependent phenomena such as stress relaxation and complex modulus and to provide a dynamic theory for mixtures of linear and branched chains. We also wish in the future to explicitly examine the results of our theory with tracer diffusion experiments.

Acknowledgment. The detailed and helpful comments from the reviewers are gratefully appreciated. Useful comments on the manuscript by R. Larson and H. Watanabe are also gratefully acknowledged. This work is supported, in part, by a NSF grant (DMR-0196033).

Appendix

Dilute Long Chain's Rouse Dynamics in Short Chain Matrix When $N_e^2 > N_S^2 > N_L$. At the end of section II.D, we mentioned the result of a long chain's dynamics in a matrix of unentangled short chains. A scaling argument is provided as followed. The diffusion constant D of a long chain in a Rouse melt involves the friction coefficient ζ as shown in eq 1, which is related to the viscosity η_s of the Rouse melt according to

$$\eta_s \simeq G\tau_R(N_S) = \zeta n_s N_S^2 b^2 \tag{A.1}$$

where the modulus $G = n_s k_B T$ with n_s being the chain number density, and τ_R is given by eq 2d. Since the segment density $c = n_s N_S \simeq 1/b^3$, we find the relation between ζ and η_s as

$$\zeta \simeq \eta_s b^3/R_S^2 \tag{A.2}$$

where $R_S = \sqrt{N_S} b$ is the end-to-end distance of a short chain. If the long chain would perform Rouse diffusion, we would have

$$D_{Rouse} \simeq \frac{k_B T}{\zeta N_L} \simeq \frac{k_B T}{\eta_s b (N_L/N_S)} \tag{A.3}$$

On the other hand, a Zimm chain would have a diffusion constant D, according to the Einstein−Stokes law, given by

$$D_{Zimm} \simeq \frac{k_B T}{\eta_s R_L} \simeq \frac{k_B T}{\eta_s N_L^{1/2} b} \tag{A.4}$$

Thus, the embedded long chain would be Rouse like if $D_{Rouse} \gg D_{Zimm}$, i.e., $N_S^2 \gg N_L$, which is the condition hypothesized previously[34] for the onset of Rouse dynamics in the dilute limit.

References and Notes

(1) de Gennes, P. G. *J. Chem. Phys.* **1971**, *55*, 572. de Gennes, P. G. *Scaling Concepts in Polymer Physics*; Cornell University Press: Ithaca, NY, 1979.
(2) Doi, M.; Edwards, S. F. *The Theory of Polymer Dynamics*, 2nd ed.; Clarendon Press: Oxford, England, 1988.
(3) Doi, M. *J. Polym. Sci., Polym. Phys. Ed.* **1983**, *21*, 667.
(4) Masuda, T.; Kitagawa, K.; Inoue, T.; Onogi, S. *Macromolecules* **1970**, *3*, 116.
(5) Prest, W. M.; Porter, R. S. *Polym. J.* **1973**, *4*, 154.
(6) Montfort, J. P.; Marin, G.; Arman, J.; Monge, P. *Polymer* **1978**, *19*, 277.
(7) Montfort, J. P.; Marin, G.; Monge, P. *Macromolecules* **1984**, *17*, 1551.
(8) Watanabe, H.; Kotaka, T. *Macromolecules* **1984**, *17*, 2316.
(9) Ylitalo, C. M.; Kornfield, J. A.; Fuller, G. G.; Pearson, D. S. *Macromolecules* **1991**, *24*, 749.
(10) Archer, J.; Archer, L. A. *J. Rheol.* **2001**, *45*, 691.
(11) Viovy, J. L.; Rubinstein, M.; Colby, R. H. *Macromolecules* **1991**, *24*, 3587.
(12) Watanabe, H. *Prog. Polym. Sci.* **1999**, *24*, 1253.
(13) McLeish, T. C. M. *Adv. Phys.* **2002**, *51*, 1379.
(14) Wasserman, S. H.; Graessley, W. W. *J. Rheol.* **1992**, *36*, 543.
(15) Frischknecht, A. L.; Milner, S. T. *J. Rheol.* **2002**, *46*, 671.
(16) Milner, S. T. *J. Rheol.* **1996**, *40*, 303.
(17) Pattamaprom, C.; Larson, R. G.; Van Dyke, T. J. *Rheol. Acta* **2000**, *39*, 517.
(18) Pattamaprom, C.; Larson, R. G. *Rheol. Acta* **2001**, *40*, 516.
(19) Tuminello, W. H. *Polym. Eng. Sci.* **1986**, *26*, 1339.
(20) Tsenoglou, C. *Macromolecules* **1991**, *24*, 1762.
(21) des Cloizeaux, J. *Macromolecules* **1990**, *23*, 4678.
(22) Yang, X.; Wang, S. Q.; Ishida, H. *Macromolecules* **1999**, *32*, 2638. Yang, X. P.; Halasa, A.; Hsu, W. L.; Wang, S. Q. *Macromolecules* **2001**, *34*, 8532.
(23) Doi, M.; Graessley, W. W.; Helfand, E.; Pearson, D. S. *Macromolecules* **1987**, *20*, 1900.
(24) Ferry, J. D. *Viscoelastic Properties of Polymers*, 3rd ed.; Wiley: New York, 1980.
(25) Klein, J. *Macromolecules* **1978**, *11*, 852.
(26) Daoud, M.; de Gennes, P. G. *J. Polym. Sci., Polym. Phys. Ed.* **1979**, *17*, 1971.
(27) Graessley, W. W. *Adv. Polym. Sci.* **1982**, *47*, 68.
(28) Struglinksi, M. J.; Graessley, W. W. *Macromolecules* **1985**, *18*, 2630.
(29) Marrucci, G. *J. Polym. Sci., Phys. Ed.* **1985**, *23*, 159.
(30) Graessley, W. W.; Edwards, S. F. *Polymer* **1981**, *22*, 1329.
(31) Colby, R. H.; Rubinstein, M. *Macromolecules* **1990**, *23*, 2753.
(32) Ball, R. C.; McLeish, T. C. B. *Macromolecules* **1989**, *22*, 1911. Milner, S. T.; McLeish, T. C. B. *Macromolecules* **1998**, *31*, 7479.
(33) Rubinstein, M. In *Theoretical Challenges in the Dynamics of Complex Fluids*; McLeish, T. C. B., Ed.; Kluwer Academic Publisher: Dordrecht, 1997.
(34) Colby, R. H. *J. Phys. II* **1997**, *7*, 93.
(35) Rubinstein, M.; Colby, R. H. *J. Chem. Phys.* **1988**, *89*, 5291.
(36) Raju, V. R.; Menezes, E. V.; Marin, G.; Graessley, W. W.; Fetters, L. J. *Macromolecules* **1981**, *14*, 1668.
(37) Tirrell, M. *Rubber Chem. Technol.* **1984**, *57*, 522.
(38) Pearson, D. S. *Rubber Chem. Technol.* **1987**, *60*, 439.
(39) Colby, R. H.; Fetters, L. J.; Funk, W. G.; Graessley, W. W. *Macromolecules* **1991**, *24*, 3873.
(40) Tao, H.; Lodge, T. P.; von Meerwall, E. D. *Macromolecules* **2000**, *33*, 1747.
(41) Fetters, L. J.; Lohse, D. J.; Richter, D.; Witten, T. A.; Zirkel, A. *Macromolecules* **1994**, *27*, 4639.

MA0210426